

SlideGen: Collaborative Multimodal Agents for Scientific Slide Generation

Xin Liang¹ Xiang Zhang² Yiwei Xu³ Siqi Sun⁴ Chenyu You¹

¹Stony Brook University ²University of British Columbia ³University of California, Los Angeles ⁴Fudan University

Generating academic slides from scientific papers is a challenging multimodal reasoning task that requires both long-context understanding and deliberate visual planning. Existing approaches largely reduce it to text-only summarization, overlooking the visual component and design-intensive nature of slide creation. In this paper, we introduce **SlideGen**, an agentic, modular, and visual-in-the-loop framework for scientific paper-to-slide generation. SlideGen orchestrates a group of vision–language agents that reason collaboratively over the document structure and semantics, producing editable PPTX slides with logical flow and compelling visual presentation. By integrating coordinated outlining, mapping, arrangement, note synthesis, and iterative refinement, our system consistently delivers slides of expert-level quality. Across diverse benchmarks and strong baselines, SlideGen outperforms existing methods in visual quality, content faithfulness, and readability, positioning it as the new state of the art in automated slide generation. Our work establishes a foundation for design-aware multi-modal slide generation, demonstrating how agentic collaboration can bridge understanding and presentation in complex multimodal reasoning tasks.

Github: <https://github.com/Y-Research-SBU/SlideGen>

Correspondence: Chenyu You: chenyu.you@stonybrook.edu

Date: December 5, 2025

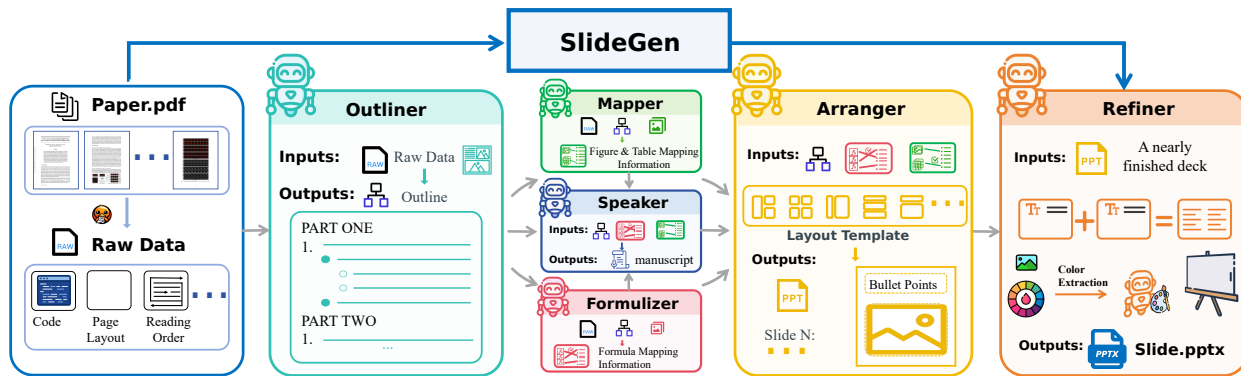


Figure 1 Overview of **SlideGen** pipeline. The multi-agent framework comprises six specialized agents that sequentially process a scientific paper via content planning, figure selection, layout design, equation integration, visual refinement, and narration generation.

1 Introduction

Creating effective academic slides from scientific papers is a complex multi-modal task. It requires condensing long, technical content into concise messages while designing visually balanced layouts that convey ideas with clarity and impact (Hu and Wan, 2013). Despite their central role in research presentations, lectures, and tutorials, slide decks are still crafted almost entirely by hand, an effort that is slow, inconsistent, and difficult to scale. Automating this process demands not only language understanding but also reasoning over visual structure, hierarchy, and design, making it a uniquely difficult problem at the intersection of vision and

language reasoning (Fu et al., 2022; Hu et al., 2025; Zhang et al., 2025a).

Recent progress in multimodal large language model (LLM) have made this automation possible, sparking a surge of interest in designing automated slides generation workflow (Sun et al., 2021; Fu et al., 2022; Bandyopadhyay et al., 2024; Xi et al., 2025; Ge et al., 2025; Xu et al., 2025; Mondal et al., 2024; Zhang et al., 2025b; Cao et al., 2025; Shi et al., 2025; Zhang et al., 2025c; Zhao et al., 2025; Zheng et al., 2025; Yang et al., 2025). Early systems like D2S (Sun et al., 2021) and Doc2PPT (Fu et al., 2022) emphasized content extraction using query-driven or hierarchical methods, with Doc2PPT adding basic layout prediction. More recent works, such as AutoPresent (Ge et al., 2025), use LLMs for programmatic control of slide elements, while PPTAgent (Zheng et al., 2025) employs an agent-like, two-stage workflow to iteratively edit slides based on analyzed reference decks.

Despite these advances, a key limitation persists: most systems focus on content assembly, often neglecting deep reasoning about visual design and cohesive layouts. For instance, AutoPresent’s precise control relies on explicit textual instructions rather than intrinsic aesthetic understanding, and many prior methods tend to produce uniform, visually repetitive layouts (see detailed comparison in Figure 3 within Section 3). Table 1 provides a comprehensive comparison of existing frameworks across key functional dimensions, revealing that no prior approach fully integrates content planning, layout reasoning, and visual refinement. Ultimately, current methods prioritize content delivery over sophisticated visual design principles and holistic presentation aesthetics.

Motivated by these limitations, we propose **SlideGen**, a modular, visual-in-the-loop, multi-agents framework that transforms scientific papers into high-quality presentation slides. As shown in Figure 1, our pipeline begins with global PDF parsing and asset extraction using DOCLING (Livathinos et al., 2025) and MARKER (Paruchuri, 2025), following (Pang et al., 2025). Six agents then operate in coordination: ❶ **Outliner** constructs the presentation structure and assigns bullet points to slides; ❷ **Mapper** and **Formulizer** attach figures, tables, and equations to their corresponding text; ❸ **Speaker** generates concise presenter notes; ❹ **Arranger** selects templates and places assets based on planned content; and ❺ **Refiner** merges sparse slides, adjusts layout consistency, and applies visual emphasis for readability.

SlideGen pioneers the integration of visual design elements into automated slide generation to combat visual fatigue and elevate presentation aesthetics. To achieve this, it employs a diverse set of layout plans from its template library, including asymmetric compositions, interleaved text-figure pairings, and alternating column structures, ensuring varied and balanced slide designs, as shown in Figure 2. This library allows users to customize templates using tools like WPS or PowerPoint, enabling them to add or modify designs by setting fonts, colors, color palettes, backgrounds, logos, and more within the slide master interface (see Appendix Figure 33 for an example of the Slide Master interface in WPS). Users can define their own master slides to match specific aesthetic preferences, making SlideGen’s templates adaptable not only for academic presentations but also for diverse themes such as educational or creative contexts. This flexibility ensures that SlideGen supports personalized, visually engaging designs tailored to varied user requirements.

To evaluate paper-to-slide generation comprehensively, we establish a standardized protocol encompassing four complementary dimensions: (i) *Visual Aesthetics* – measured by *geometry-aware density (GAD) score* rewarding layouts that are neither sparse nor cluttered; (ii) *Communication Effectiveness* – assessed by SlideQA, which tests how well the generated slides support question answering (Pang et al., 2025); (iii) *Holistic Quality* – evaluated by VLM-as-Judge over Content, Design, and Coherence (Zheng et al., 2025); and (iv) *Textual Coherence* – reflecting fluency and clarity of written expressions. Our main contributions are as follows: 1) We introduce **SlideGen**, a modular, agentic framework for automatic paper-to-presentation generation that plans structure, aligns multi-modal content, and yields visually coherent slides without any reference decks; 2) We propose geometry-aware density (GAD) score, a quantitative measure of aesthetic balance that correlates strongly with human preferences; 3) We provide an extensible layout-template library that supports diverse and customizable slide patterns for flexible composition. We release our code, template library, and evaluation scripts in the supplementary material.

Table 1 Selected comparison of automatic slide generation systems. This table summarizes selected objective capabilities of existing approaches for a concise overview (see Table 3 for comprehensive details).

| Framework | Content Struct. | Text–Fig Align. | Multi Modal | Output Format | User Editability |
|--|-----------------|-----------------|-------------|---------------|------------------|
| PPSGen (2013) (Hu and Wan, 2013) | ○ | ✗ | ✗ | text | ✗ |
| D2S (2021) (Sun et al., 2021) | ○ | ✓ | ✓ | text | ✗ |
| DOC2PPT (2022) (Fu et al., 2022) | ✓ | ✓ | ✓ | PPTX/PDF | ✗ |
| Persona-Aware D2S (2024) (Mondal et al., 2024) | ✓ | ○ | ✓ | PDF | ✗ |
| GDP (2024) (Maheshwari et al., 2024) | ✓ | ✗ | ✗ | text | ✗ |
| DocPres (2024) (Bandyopadhyay et al., 2024) | ✓ | ○ | ✓ | PDF | ✗ |
| PASS (2025) (Aggarwal and Bhand, 2025) | ✓ | ○ | ✓ | PPTX | ✗ |
| RCPS (2025) (Xi et al., 2025) | ✓ | ✓ | ✓ | PPTX/PDF | ✗ |
| PPTAgent (2025) (Zheng et al., 2025) | ✓ | ✓ | ✓ | PPTX/HTML | ✓ |
| Auto-Slides (2025) (Yang et al., 2025) | ✓ | ✓ | ✓ | PDF | ✗ |
| AutoPresent (2025) (Ge et al., 2025) | ✗ | ○ | ✓ | PPTX | ✗ |
| SlideGen (Ours) | ✓ | ✓ | ✓ | PPTX | ✓ |

2 Related Work

Vision-Language Agents for Slides. Early document-to-slide systems treated slide making as text generation, either query-based single-document summarization (Sun et al., 2021; Cao et al., 2025) or sequence-to-sequence mapping from sections to slides (Fu et al., 2022; Kothawade et al., 2020). With the rise of VLMs, research on automatic document-to-slide generation has shifted from single-shot prompting to multi-agent, multi-stage pipelines (OpenAI et al., 2024; Zhang et al., 2025d, 2022; Wei et al., 2025a; Naveed et al., 2025). Representative work decompose the task into planning and grounding (Wei et al., 2025b), where *DocPres* (Bandyopadhyay et al., 2024) separates global summarization, outline drafting, and slide-section grounding, *RCPS* (Xi et al., 2025) assigns specialized roles for global planning, layout planning, and iterative refinement, and (Xu et al., 2025) improves layout fidelity via a Reviewer-Refiner loop.

Among high-performing baselines, *PPTAgent* (Zheng et al., 2025) uses a two-stage, edit-based pipeline over HTML layouts with self-correction, but it (i) relies on explicit references for layout editing, (ii) tends to layout problems, which include element overlap and text overflow. In contrast, **SlideGen** is a visual-in-the-loop multi-agent pipeline: it grounds an explicit outline to layouts, maps figures and equations precisely, composes pages from an extensible template library, and targets balanced density across pages, which is validated by our geometry-aware density metric. In practice, this extensible template library serves as a generalized summary of many reference decks, effectively playing the role of innumerable references while remaining compact and generalizable.

Evaluation Protocols and Metrics for Slides. Evaluation has evolved from text-only measures to multimodal, narrative-aware protocols. Early methods primarily relied on n-gram overlap (ROUGE) and language-model fluency (perplexity) to assess slide text (Sun et al., 2021; Fu et al., 2022; Lin, 2004; Jelinek et al., 1977). More recent work moves beyond pure text metrics. Researchers add multimodal, source-grounded factual QA with questions extracted from original paper. Evaluations also use VLMs on slide renderings to assess layout design, readability, and narrative flow (Pang et al., 2025; Zheng et al., 2025; Zhang et al., 2023; Sun et al., 2025; Shi et al., 2025). While VLM-as-judge covers content fidelity, design, and narrative coherence (Bandyopadhyay et al., 2024; Zheng et al., 2025; Pang et al., 2025; Xiong et al., 2025; You et al., 2025; Xi et al., 2025; Shi et al., 2025), these scores can be prompt- and model-dependent, and traditional text metrics largely ignore visual layout aesthetics, including occupancy, overlap, fragmentation. We therefore define a geometry-aware density (GAD) score, a layout-centric metric that quantifies page occupancy, overlap, and fragmentation to assess visual organization and aesthetics. We further validate the GAD score against human ratings.

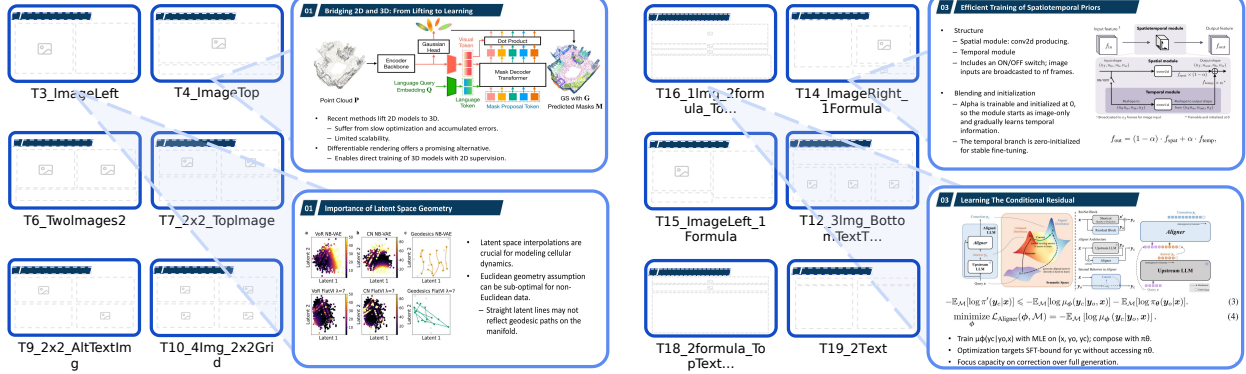


Figure 2 Overview of the template library and representative slide outputs. The left and right panel follow the same structure: the left side shows a subset of the slide template library used by Arranger; the right side shows two representative slides generated with those templates. Four slides are shown in total, produced with templates T3, T4, T14, and T16. Each template addresses a typical presentation structure (e.g., text-only, image-left, two-column). Throughout the paper, we adopt 16:9 as the default deck aspect ratio, while users are free to modify the template library’s size and aspect ratio. The complete collection is provided in the Appendix Section F.

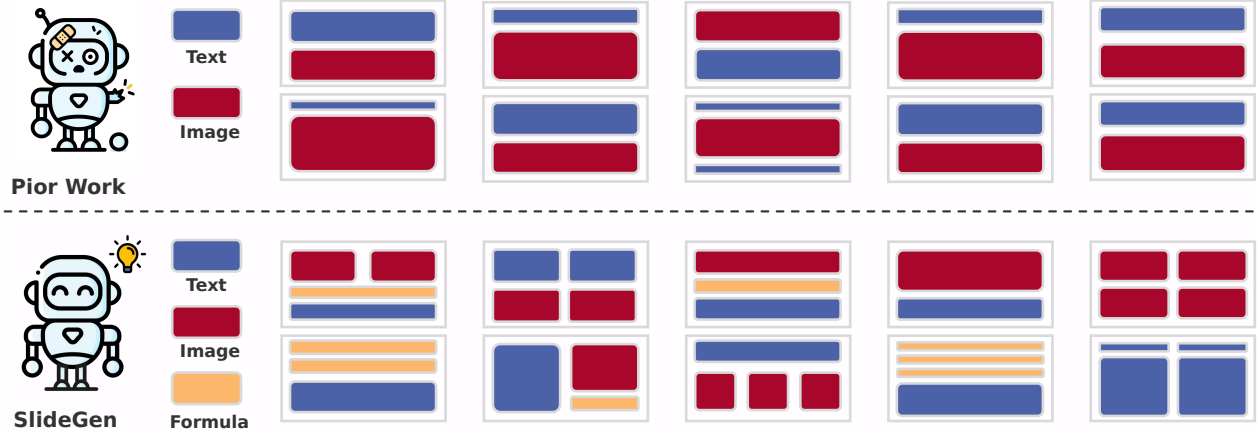


Figure 3 Comparison of generated slides with block abstractions. Each slide is shown as colored blocks, revealing that prior methods largely converge to similar vertical layouts, while **SlideGen** produces more varied and visually structured designs.

3 SlideGen

Overview. SlideGen is a modular, multimodal-agentic framework that turns scientific papers into structured and well-designed editable PPTX slides. It first extracts and organizes the paper’s content into an explicit slide outline, then plan each slide page generation as a visual reasoning process that maximizes readability and information density. As shown in Figure 1, our framework is organized into six specialized agents, each responsible for a different stage of generation.

Figure 3 compares representative layouts produced by different methods. For prior work, we intentionally visualize only their strongest layouts and omit obvious failure cases with large blank regions, cluttered text, or overlapping elements, so that the comparison is based on relatively strong visual cases.

Even when we only show relatively strong layouts from prior work, our approach still delivers more visually engaging slide designs. Existing methods tend to stack content from top to bottom in simple text–image blocks, resulting in visually flat, repetitive layouts with limited visual structure. In contrast, SlideGen introduces an extensible library of 19 layout templates that support richer, asymmetric compositions, such as left–right text–figure pairings, interleaved equations, and alternating column structures. This design space allows SlideGen to make better use of horizontal space, create clearer visual grouping, and produce pages

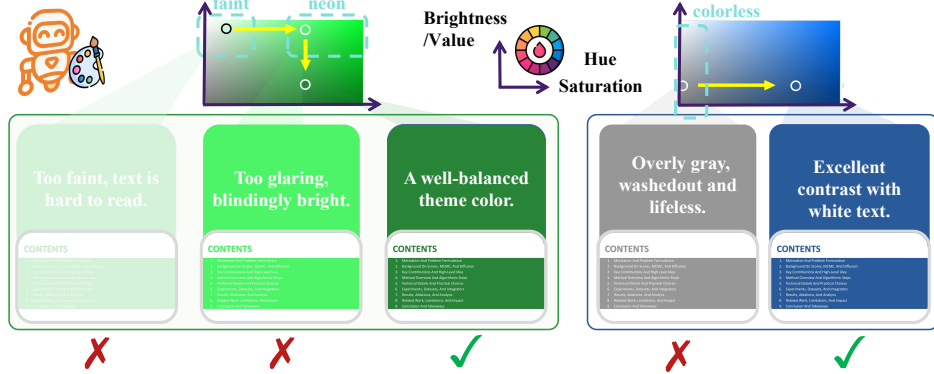


Figure 4 Color adjustment method on two fixed-hue planes for Refiner. Examples on the left and right illustrate failure cases and the final readable and high-contrast choice.

that look more balanced, diverse, and polished across the entire deck.

Preprocessing. We first preprocess the raw PDF by converting pages to Markdown and assembling a library consisting of two modalities: (i) text assets capture the hierarchy by mapping each section heading to its corresponding paragraph-level content stored as key-value pairs, and (ii) visual assets map figure and table captions to the extracted image files. We next describe the design of each of the six LLM agents in the following.

Outliner. Outliner reads the entire document, identifies key ideas and dependencies based on strong language understanding abilities of LLMs, and produces a two-level presentation outline.

As shown in Appendix Figure 43, it returns a structured JSON-like object with two top-level keys: `metadata` and `sections`. `metadata` records the paper title, author names, the publication date, and the organization. The `sections` part is an ordered list that follows a recommended narrative: motivation and background, related work or limitations, key contributions, method overview, technical details, experiments and datasets, results and analysis, optional ablations/insights, and conclusion and future work. Outliner applies this template case by case: it may split long topics into two sections to keep each section focused on one topic, or fold minor topics into the most relevant neighboring section to improve coherence, so the final sectioning varies across papers. Once the high-level outline is fixed, Outliner refines the plan at the slide level. For each section, it introduces one or more subsections as needed and maps them to one slide titles. For each slide, it proposes a concise title and a short summary, preserving logical dependencies and avoiding redundancy.

Mapper. After Outliner identifies and allocates content to slides, Mapper links each figure or table to the slide(s) it best supports. As shown in Appendix Figure 56, it outputs a JSON file that records, for every visual asset, the target slide index and a brief explanation of why the asset supports that slide. A single asset may be reused across multiple slides when appropriate, and assets that do not materially support the narrative are left unassigned.

Formulizer. Building on Outliner’s section plan, Formulizer extracts mathematical formulas from the paper and maps each one to the most relevant section. For every formula it records a normalized representation (LaTeX or an image crop), the target section, and a brief explanation based on the surrounding text. Conceptually similar to Mapper but specialized for equations, Formulizer supports three ways to obtain formula data: (i) detect formula bounding boxes in the PDF and crop them directly, reusing the image-asset pipeline; (ii) extract the LaTeX code of formulas and render them. However, the rendered output may not always perfectly match the original formula, especially in terms of spacing, font, or stylistic nuances, leading to potential rendering crashes and errors; (iii) allow the user to draw bounding boxes on the source file, after which only those regions are processed, explained, and placed on the corresponding slides. Method (iii) provides an interactive, human-in-the-loop approach, making it the most precise option for content selection. By default, we use method (i) bounding-box detection and cropping.

Arranger. With Outliner’s section plan and the asset mappings from Mapper and Formulizer prepared, Arranger determines how it is organized and presented. It selects a suitable layout template based on the

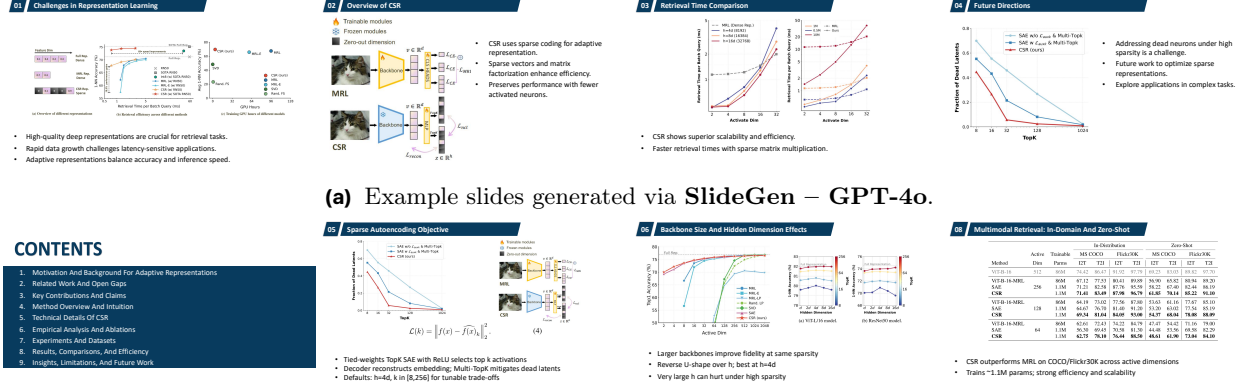


Figure 5 Example slides generated via **SlideGen** using GPT-4o (a) and GPT-5 (b) with the default deep blue theme. Additional samples are shown in Appendix Section D. We use structured prompt templates for all agent calls, and the full prompts for all agents are provided in Appendix Section G.

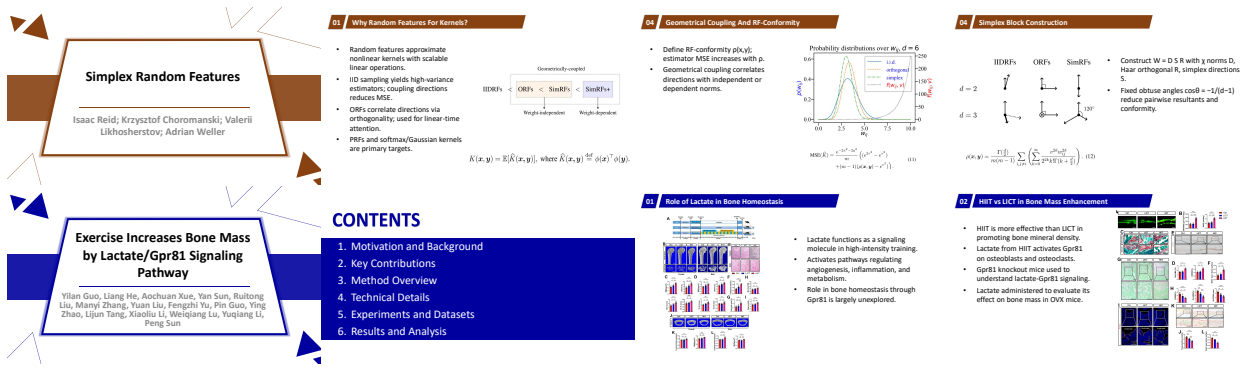


Figure 6 Example slides generated via **SlideGen** with the theme refined by Refiner. Slides in the second row come from a biomedical paper.

number and types of elements, and on the size and aspect ratio of the visuals.

To support layout assignment and precise placement, we introduce a compact and extensible library of slide templates that covers nearly all common presentation patterns. As illustrated in Figure 2, the library includes text-only, image-left/right, two-image, three-image, four-image, and formula-strip layouts. Using this library, Arranger selects an appropriate template that matches the content. For example, slides containing a prominent, wide-aspect image with a few sentences of text tends to be assigned to the T4 image-top template; when the main image is tall or nearly square, Arranger prefers a half-and-half image-text layout such as T2 image-right or T3 image-left. By decoupling layout selection from content generation, Arranger ensures slides are informative, visually balanced, and consistent with good presentation practice. It produces an almost complete deck, which is then handed to Refiner for final adjustments. A complete example appears in Appendix Section H.

Refiner. Refiner polishes the deck for clarity and cohesion and applies a unified theme color. It performs two main tasks: (i) **Slide consolidation**. Consecutive textual slides without any visuals, are merged to reduce redundancy and keep the narrative concise. When two text-only slides are merged, Refiner switches the layout to T19-2Text. (ii) **Color Setting**. Refiner derives a base color from the paper’s figures and adjusts it to serve as the deck’s theme. There are three steps for base color extraction: (i) collect pixels from images, ignoring near-transparent pixels so that transparency is not mistaken for black. (ii) remove near-white and near-black pixels based on brightness, so that large bright backgrounds and deep shadows

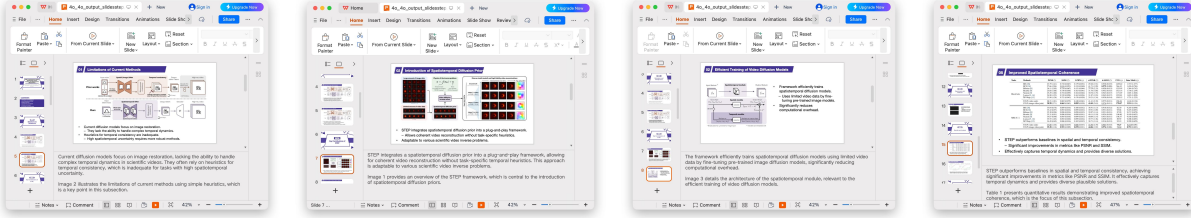


Figure 7 Example slides generated via **SlideGen** with speaking notes, shown as screenshots taken from WPS. More examples with speaking notes are provided in Appendix Figure 14.

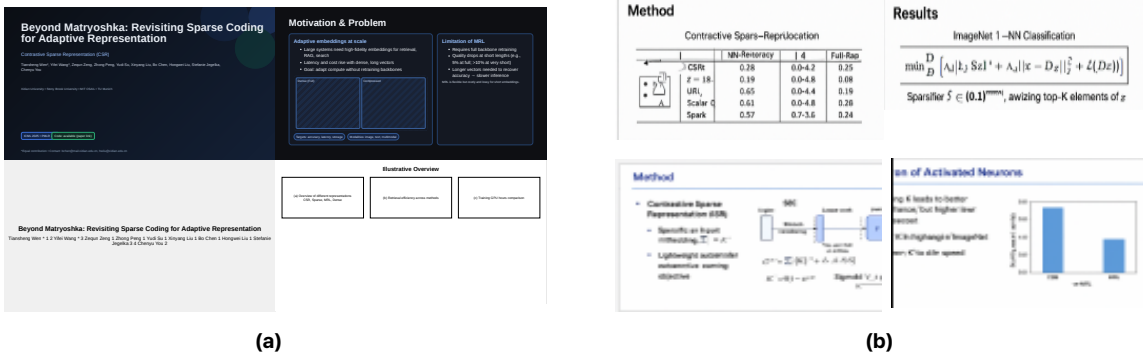


Figure 8 Baselines for slide generation. Four representative baselines are shown. (a) Example slides webpage rendered from ChatGPT-generated HTML code (top row: GPT-5, bottom row: GPT-4o). (b) Example slides generated via the website’s Question&Answer ChatGPT (top row: GPT-5, bottom row: GPT-4o). More samples gerated by baselines are shown in Appendix Section E.

do not dominate the statistics. (iii) among the remaining pixels, count exact 24-bit RGB values and choose the most frequent one as the base color. In practice, the raw base color is often too faint for a presentation theme, as shown in the left panel of Figure 4, which can hurt text readability. Refiner therefore refines the color on a fixed-hue HSV plane using a simple rule: first move right to make the color more vivid, but not garish, then move down to make it appropriately dark for a presentation theme. If the color becomes slightly too dark, we apply a small safety lift. When the base color is near gray and the hue is unstable, we lock the hue to a deep blue palette anchor and raise saturation, the right panel of Figure 4 illustrates the effect. Further implementation details for color setting are provided in Appendix Section I.

Speaker. Leveraging Outliner’s subsection structure, Speaker generates a coherent spoken script with one paragraph per subsection. As shown in Appendix Figure 53, it produces notes that maps each subsection to a 2–5 sentence, presentation-ready paragraph that is factual and concise. In addition, Speaker directly incorporates the placement rationales from Mapper (figures/tables) and Formulizer (equations), appending them in the notes of the corresponding slides. Visual examples of speaking notes generated by Speaker can be seen in Figure 14.

4 Experiment

Dataset Source. We curated a domain-specific dataset focused on recent advances in machine learning and natural language processing, with a particular emphasis on research diversity and quality. Our dataset consists of 200 peer-reviewed papers collected from leading AI venues between 2022 and 2025, including only Oral presentations as designated by each conference. A detailed breakdown by venue and year is provided in Appendix Table 6.

Notations. Let a deck comprises N slides, denoted $(s_i)_{i=1}^N$. Each slide has a role $r_i \in \{\text{title}, \text{agenda}, \text{content}, \text{thanks}\}$. We consider a fixed slide layout: slide s_1 is the **title** page, slide s_2 is the **agenda** page, slides s_3, \dots, s_{N-1}

Table 2 Results table combining SlideQA metrics (Verbatim, Interpretive, Overall) with Perplexity, Density (OM, FR, D-Avg), and VLM-as-Judge (Content, Design, Coherence, Avg).

| Model | Verbatim \uparrow | | | Interpretive \uparrow | | | Overall | PPL \downarrow | Density \uparrow | | | VLM-as-Judge \uparrow | | | |
|-----------------|---------------------|--------------|--------------|-------------------------|--------------|--------------|--------------|------------------|--------------------|--------------|--------------|-------------------------|-------------|-------------|-------------|
| | open-src | closed-src | V-Avg | open-src | closed-src | I-Avg | | | OM | FR | D-Avg | Content | Design | Coherence | Avg |
| <i>GPT-5</i> | | | | | | | | | | | | | | | |
| HTML-5 | 74.95 | 70.17 | 72.56 | 84.24 | 87.88 | 86.06 | 79.31 | 189.38 | 54.32 | 60.66 | 56.86 | 3.54 | 4.02 | 4.09 | 3.88 |
| Image-5 | 66.99 | 53.90 | 60.45 | 73.06 | 80.51 | 76.79 | 68.62 | 605.02 | 67.96 | 79.29 | 72.49 | 2.84 | 3.16 | 3.21 | 3.07 |
| PPTAgent-5 | 61.37 | 63.21 | 62.29 | 75.22 | 78.55 | 76.89 | 69.59 | 450.12 | 55.32 | 62.40 | 58.15 | 3.10 | 3.25 | 3.40 | 3.25 |
| PosterAgent-5 | 70.08 | 78.98 | 74.53 | 82.21 | 85.34 | 83.78 | 79.15 | 220.75 | 62.42 | 70.28 | 65.56 | 3.45 | 3.60 | 3.75 | 3.60 |
| Ours-5 | 75.70 | 70.05 | 72.88 | 84.65 | 90.36 | 87.51 | 80.19 | 48.40 | 69.08 | 84.56 | 75.27 | 4.12 | 4.30 | 4.35 | 4.26 |
| <i>GPT-4o</i> | | | | | | | | | | | | | | | |
| HTML-4o | 60.48 | 75.58 | 68.03 | 87.38 | 91.37 | 89.38 | 78.70 | 200.79 | 41.15 | 46.38 | 43.24 | 3.02 | 2.76 | 3.97 | 3.25 |
| Image-4o | 48.97 | 30.85 | 39.91 | 50.11 | 70.72 | 60.42 | 50.16 | 793.71 | 75.28 | 76.24 | 75.66 | 2.39 | 3.09 | 3.50 | 2.99 |
| PPTAgent-4o | 57.99 | 52.44 | 55.22 | 57.51 | 56.34 | 56.93 | 56.07 | 721.54 | 53.27 | 56.31 | 54.49 | 3.25 | 3.24 | 3.29 | 3.26 |
| PosterAgent-4o | 67.75 | 67.86 | 67.81 | 72.99 | 79.89 | 76.44 | 72.12 | 139.67 | 68.76 | 76.25 | 71.76 | 3.19 | 3.48 | 4.53 | 3.73 |
| Ours-4o | 75.89 | 71.23 | 73.56 | 90.60 | 93.89 | 92.25 | 83.90 | 50.59 | 79.66 | 82.32 | 80.99 | 4.01 | 4.28 | 4.66 | 4.32 |
| <i>Qwen</i> | | | | | | | | | | | | | | | |
| PosterAgent-7B | 49.74 | 47.43 | 48.59 | 54.30 | 56.25 | 55.28 | 51.93 | 450.30 | 42.48 | 49.11 | 45.13 | 2.41 | 2.69 | 2.84 | 2.65 |
| SlideGen-7B | 55.52 | 53.10 | 54.31 | 60.83 | 63.16 | 62.00 | 58.15 | 180.50 | 46.61 | 54.02 | 49.57 | 2.70 | 2.95 | 3.12 | 2.92 |
| PosterAgent-72B | 58.97 | 56.32 | 57.65 | 65.29 | 68.88 | 67.09 | 62.37 | 150.60 | 49.35 | 57.42 | 52.58 | 2.92 | 3.13 | 3.30 | 3.12 |
| SlideGen-72B | 62.74 | 60.59 | 61.67 | 72.14 | 74.51 | 73.33 | 67.50 | 80.90 | 52.31 | 60.56 | 55.61 | 3.10 | 3.32 | 3.54 | 3.32 |

are **content** pages, and the last slide s_N is **thanks** page. Formally, a deck has N slides $\{s_i\}_{i=1}^N$ with roles $r_1 = \text{title}$, $r_2 = \text{agenda}$, $r_i = \text{content}$, for $3 \leq i \leq N-1$, and $r_N = \text{thanks}$. The content page contains agenda items (“PART 1/2, …”). Let $\mathcal{A} = [a_1, \dots, a_m]$ be the ordered list of top-level bullets on s_2 .

Evaluation Metrics. We evaluate this Paper-to-Slide task with four complementary metrics, covering (i) layout quality (GAD), (ii) deck-only answerability (SlideQA), (iii) overall presentation quality across **Content**, **Design** and **Coherence** (VLM-as-Judge), and (iv) textual coherence (writing and flow). More detailed definitions and evaluation protocols for each metric are provided in Appendix Section A.

Visual Aesthetics. We propose the *Geometry-Aware Density (GAD) score* to quantify layout aesthetics and readability. It evaluates layout density while also considering visually pleasing and comfortable design for human through two components: (i) **Area Occupancy**: This measures how much of the slide’s space is used, comparing it to a target occupancy value τ . If the slide is too empty or too full, it negatively impacts the score. (ii) **Effective Region Count**: the number of non-trivial content regions on a slide, where a region is counted only if its area exceeds a minimum gate $a_{\min} > 0$. Let M_i^{eff} denote this count for slide i .

We define a downward-opening quadratic fragmentation reward with maximum at M^* :

$$R_i^{\text{frag}} = \max \left\{ 0, 1 - \frac{(M_i^{\text{eff}} - M^*)^2}{\kappa} \right\} \in [0, 1]. \quad (4.1)$$

Occupancy matching and fragmentation rewards are:

$$\text{OM}_i \triangleq 1 - |\rho_i - \tau|, \quad \text{FR}_i \triangleq R_i^{\text{frag}}. \quad (4.2)$$

The per-slide geometry score are:

$$s_i^{\text{geom}} = \lambda_1 \text{OM}_i + \lambda_2 \text{FR}_i, \quad \lambda_1 + \lambda_2 = 1. \quad (4.3)$$

At the deck level with N slides, we average per-slide scores to obtain:

$$\text{GAD}^{\text{geom}} = \frac{1}{N} \sum_{i=1}^N (\lambda_1 \text{OM}_i + \lambda_2 \text{FR}_i). \quad (4.4)$$

Holistic Assessment. Following PPTEVAL (Zheng et al., 2025), we evaluate decks along three dimensions – **Content**, **Design** and **Coherence**, using GPT-4o as the judge. Scores range from 1–5 and are accompanied by brief rationales. The criteria are listed in Appendix Table 5.

Communication Effectiveness. Since slide decks are the primary vehicle by which speakers convey knowledge and audiences learn it, we need to evaluate whether our generated presentations communicate the material, and how much they succeed in doing so. Following PaperQuiz (Pang et al., 2025), for each paper,

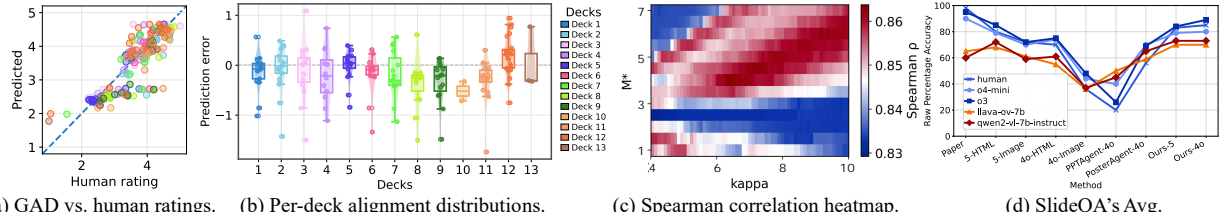


Figure 9 Overview of quantitative results (Leave-One-Deck-Out and human eval). (a) **Prediction vs. human ratings.** Each point is one page. The dashed line is $y = x$ and indicates perfect agreement. We report RMSE, Pearson’s r , and Spearman’s ρ . Metrics are computed across all test pages from 13 decks, about 750 pages in total. Here: RMSE = 0.580, $\rho = 0.820$, $r = 0.811$. (b) **Per-deck alignment distributions:** The page-wise errors $\hat{y} - y$ are summarized by the median, interquartile range (IQR), and $1.5 \times \text{IQR}$. The dashed line at 0 indicates unbiased predictions. (c) **Spearman correlation heatmap** over the parameter space (M^* , κ) on the human-rated pages. The heatmap visualizes the correlation between the predicted and human ratings for different combinations of M^* and κ , with brighter areas indicating higher Spearman correlation (i.e., better alignment with human ratings). The optimal parameters are selected based on the peak correlation. (d) **Average SlideQA scores** for each reader (colored lines) across slides generated by different methods (x-axis). See Appendix Section C for the full model names.

we first generate a quiz of 100 questions from the paper PDF: 50 verbatim questions answerable directly from the text, covering diverse factual aspects, and 50 interpretive questions targeting higher-level comprehension. Then the questions are answered by six different VLM readers.

Textual Coherence. We quantify textual coherence using the standard “Perplexity” (PPL) metric, calculated for the entire slide text under Llama-2-7b-hf. A lower PPL score indicates more predictable and coherent language, see details in Appendix Section A.5.

4.1 Baselines and Settings

We evaluate our framework on multi slide PowerPoint generation with a 16:9 canvas, the number of slides is unconstrained. The compared baselines span three categories: (i) *end to end generators*: GPT-5 HTML and GPT-4o HTML, which generate HTML+CSS code for slides, and GPT-5 Image and GPT-4o Image, which directly synthesize slide images page by page; (ii) *multi agent workflows*: PPTAgent-4o, PPTAgent-5, PosterAgent-4o, PosterAgent-5, and PosterAgent-qwen 2.5 VL 7B&72B, used in *slide mode*, which decompose planning, drafting, and layout into iterative editing steps; and (iii) our method instantiated with two backbones, GPT-4o and GPT-5, enabling a controlled comparison across backbones while keeping the rest of the pipeline unchanged.

All methods take the same source PDF per paper. We report *accuracy* on SlideQA, distinguishing between Verbatim and Interpretive questions; overall *PPL* over concatenated slide text; and *Geometry Aware Density* with its two components, *Occupancy Match* and *Fragmentation Reward*; together with *VLM-as-Judge* scores along *Content*, *Design* and *Coherence*. Exact metric definitions are given in Section 4.

4.2 Results

4.2.1 Overall Performance vs. baselines

As shown in Table 2, Ours-4o delivers the strongest overall score in the table, improving over the best GPT-4o baseline, while maintaining very competitive interpretive performance without sacrificing verbatim coverage. This suggests our pipeline lifts detail retention without sacrificing global readability. On the GAD score, our generated decks are neither overly sparse nor cluttered compared with those from the baselines. Figure 5 and 6 show slides generated by **SlideGen** with GPT-4o and GPT-5, while Figure 8 illustrates four representative baseline systems for comparison. We also observe that GPT-Image achieves noticeably higher GAD scores than GPT-HTML. This suggests that, although the rendered images can be slightly blurry, the GPT-Image pipeline still tends to produce comfortable, well-spaced layouts overall, whereas GPT-HTML, despite generating perfectly readable content, often results in layouts that feel less visually comfortable and less appealing.

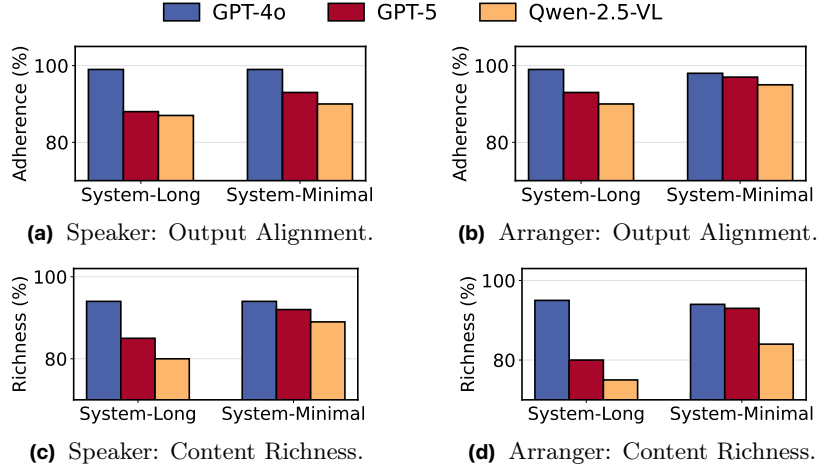


Figure 10 Backbone-specific prompt structure sensitivity. The top row shows Output Alignment (percentage of outputs adhering to the required format) for Speaker and Arranger under two prompt structures. The bottom row shows Content Richness (percentage of total content generated, normalized by model-specific baselines) for the same tasks and prompt structures.

4.2.2 Alignment with Human Judgments

GAD Aligns with Human Preferences. We evaluate the GAD metric by calibrating it against human ratings. 40 raters scored 13 decks each on a 1–5 scale. Using these ratings, we selected optimal hyperparameters $M^* = 4$ and $\kappa = 6.3$ via grid search, maximizing the Spearman correlation, as shown in Figure 9(c). The calibration is performed with an affine function:

$$\hat{y} = a + b_1 \text{OM} + b_2 \text{FR} \quad (4.5)$$

where OM and FR are the geometry features.

The results of this calibration are shown in Figure 9. Further details on the calibration process are provided in the Appendix Section A.3.

SlideQA Human Check. To assess our SlideQA method with human judgment, we recruited 5 PhD student to complete the SlideQA on 5 randomly selected papers from our dataset. The average score of these 5 PhD students represents the human reader in our evaluation. For each paper, we evaluated 8 methods in total, including 6 baselines and 2 variants of our method, following the setup in Section 4.1. As shown in Figure 9(d), there is good consistency between the human and the VLM readers. This alignment supports the use of reader models as effective proxies for human judgment.

4.2.3 Insights & Ablations

Backbone Variants and Prompt Sensitivity. Comparing our two backbones, Ours-4o outperforms Ours-5 on end-to-end pipeline metrics. While GPT-5 shows stronger code synthesis, it also exhibits higher execution-failure and greater sensitivity to prompt phrasing. Prompts that succeed with GPT-4o are sometimes misinterpreted by GPT-5. To mitigate this, we tighten the system prompt and enforce a stricter JSON output schema, separating a minimal system intent from a template-defined output specification. A controlled study of prompt structure confirms GPT-5’s sensitivity and quantifies the gains from this design (see Figure 10, Appedix Section B.2). With the refined prompt, GPT-5 yields valid, format-compliant outputs more reliably while preserving controllability.

Across our dataset, GPT-5 variants typically produce more sections than GPT-4o yet include fewer sub-bullet points within each section, revealing different outlining preferences rather than uniform increases in detail.

Interpretive vs. Verbatim Gap. Across all methods, interpretive accuracy is consistently and substantially higher than verbatim accuracy, as reflected in the SlideQA results reported in Table 2. This gap is large for most methods. The pattern indicates that fine-grained, quote-level details are harder to preserve and retrieve in multi-slide PPT generation than high-level understanding and reasoning. In practice this is

expected: slides compress text, distribute content over multiple pages, and often replace long sentences with bullets or figures, thereby preserving the gist while reducing exact quote-level matches.

HTML Routes Outperform Image-only Routes. Using GPT to produce HTML/CSS significantly outperforms using it to produce pixel-based images. Image-only generation renders text as pixels, so it cannot be directly extracted and must rely on OCR. Because many “characters” are merely drawn, stroke-like approximations rather than standard glyphs, they often exhibit missing strokes, unintended joins, and distortions, which raise OCR error rates and further hinder content recognition. By contrast, HTML-based generation preserves actual text and layout structure, and the gap in readability and parseability between the two is substantial.

4.2.4 Efficiency & Cost

We analyze **SlideGen** at the agent level by measuring wall-clock time, input tokens, and output tokens for each agent call, as shown in Figure 11. We find that the GPT-4o variant costs slightly more but runs faster, see details in Appendix Section B.

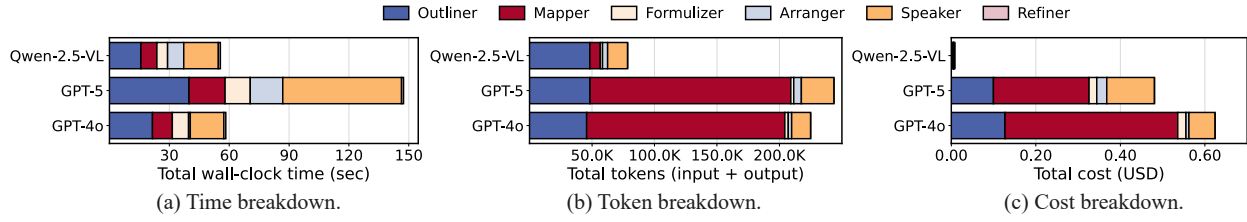


Figure 11 Agent-level efficiency and cost. Horizontal stacked bars per variant show per-agent contributions to (a) time, (b) tokens, and (c) cost.

5 Conclusions

We propose **SlideGen**, a step-by-step framework that covers outline planning, asset grounding, template selection, speaker-note drafting, and global refinement. We also introduce evaluation protocols including Geometry-Aware Density, VLM-as-Judge, SlideQA, and Textual Coherence. **SlideGen** advances automated slide generation toward human quality and improves efficiency, enabling practical, scalable scientific communication.

References

Yue Hu and Xiaojun Wan. Ppsgen: Learning to generate presentation slides for academic papers. In *IJCAI*, pages 2099–2105, 2013.

Tsu-Jui Fu, William Yang Wang, Daniel McDuff, and Yale Song. Doc2ppt: Automatic presentation slides generation from scientific documents. In *Proceedings of the AAAI Conference on Artificial Intelligence*, pages 634–642, 2022.

Ming Hu, Chenglong Ma, Wei Li, Wanghan Xu, Jiamin Wu, Jucheng Hu, Tianbin Li, Guohang Zhuang, Jiaqi Liu, Yingzhou Lu, et al. A survey of scientific large language models: From data foundations to agent frontiers. *arXiv preprint arXiv:2508.21148*, 2025.

Xiang Zhang, Juntai Cao, Chenyu You, and Dujian Ding. Why prompt design matters and works: A complexity analysis of prompt search space in llms. In *Proceedings of the 63rd Annual Meeting of the Association for Computational Linguistics (Volume 1: Long Papers)*, pages 32525–32555, 2025a.

Edward Sun, Yufang Hou, Dakuo Wang, Yunfeng Zhang, and Nancy XR Wang. D2s: Document-to-slide generation via query-based text summarization. *arXiv preprint arXiv:2105.03664*, 2021.

Sambaran Bandyopadhyay, Himanshu Maheshwari, Anandhavelu Natarajan, and Apoorv Saxena. Enhancing presentation slide generation by llms with a multi-staged end-to-end approach. *arXiv preprint arXiv:2406.06556*, 2024.

Wang Xi, Quan Shi, Tian Yu, Yujie Peng, Jiayi Sun, Mengxing Ren, Zenghui Ding, and Ningguang Yao. Multi-agent synergy-driven iterative visual narrative synthesis. *arXiv preprint arXiv:2507.13285*, 2025.

Jiaxin Ge, Zora Zhiruo Wang, Xuhui Zhou, Yi-Hao Peng, Sanjay Subramanian, Qinyue Tan, Maarten Sap, Alane Suhr, Daniel Fried, Graham Neubig, et al. Autopresent: Designing structured visuals from scratch. In *Proceedings of the Computer Vision and Pattern Recognition Conference*, pages 2902–2911, 2025.

Yunqing Xu, Xinbei Ma, Jiyang Qiu, and Hai Zhao. Textual-to-visual iterative self-verification for slide generation. *arXiv preprint arXiv:2502.15412*, 2025.

Ishani Mondal, S Shwetha, Anandhavelu Natarajan, Aparna Garimella, Sambaran Bandyopadhyay, and Jordan Boyd-Graber. Presentations by the humans and for the humans: Harnessing llms for generating persona-aware slides from documents. In *Proceedings of the 18th Conference of the European Chapter of the Association for Computational Linguistics (Volume 1: Long Papers)*, pages 2664–2684, 2024.

Xiang Zhang, Juntai Cao, Jiaqi Wei, Yiwei Xu, and Chenyu You. Tokenization constraints in llms: A study of symbolic and arithmetic reasoning limits. *arXiv preprint arXiv:2505.14178*, 2025b.

Juntai Cao, Xiang Zhang, Raymond Li, Jiaqi Wei, Chuyuan Li, Shafiq Joty, and Giuseppe Carenini. Multi2: Multi-agent test-time scalable framework for multi-document processing. In *Proceedings of The 5th New Frontiers in Summarization Workshop*, pages 135–156, 2025.

Jingwei Shi, Zeyu Zhang, Biao Wu, Yanjie Liang, Meng Fang, Ling Chen, and Yang Zhao. Presentagent: Multimodal agent for presentation video generation. *arXiv preprint arXiv:2507.04036*, 2025.

Xiang Zhang, Tianze Ling, Zhi Jin, Sheng Xu, Zhiqiang Gao, Boyan Sun, Zijie Qiu, Jiaqi Wei, Nanqing Dong, Guangshuai Wang, et al. π -primenovo: an accurate and efficient non-autoregressive deep learning model for de novo peptide sequencing. *Nature Communications*, 16(1):267, 2025c.

Haokun Zhao, Xiang Zhang, Jiaqi Wei, Yiwei Xu, Yuting He, Siqi Sun, and Chenyu You. Timeseriesscientist: A general-purpose ai agent for time series analysis. *arXiv preprint arXiv:2510.01538*, 2025.

Hao Zheng, Xinyan Guan, Hao Kong, Jia Zheng, Weixiang Zhou, Hongyu Lin, Yaojie Lu, Ben He, Xianpei Han, and Le Sun. Pptagent: Generating and evaluating presentations beyond text-to-slides. *arXiv preprint arXiv:2501.03936*, 2025.

Yuheng Yang, Wenjia Jiang, Yang Wang, Yiwei Wang, and Chi Zhang. Auto-slides: An interactive multi-agent system for creating and customizing research presentations. *arXiv preprint arXiv:2509.11062*, 2025.

Nikolaos Livathinos, Christoph Auer, Maksym Lysak, Ahmed Nassar, Michele Dolfi, Panos Vagenas, Cesar Berrospí Ramis, Matteo Omenetti, Kasper Dinkla, Yusik Kim, et al. Docling: An efficient open-source toolkit for ai-driven document conversion. *arXiv preprint arXiv:2501.17887*, 2025.

Vik Paruchuri. Marker: Convert pdf to markdown and json quickly with high accuracy, 2025.

Wei Pang, Kevin Qinghong Lin, Xiangru Jian, Xi He, and Philip Torr. Paper2poster: Towards multimodal poster automation from scientific papers. *arXiv preprint arXiv:2505.21497*, 2025.

Himanshu Maheshwari, Sambaran Bandyopadhyay, Aparna Garimella, and Anandhavelu Natarajan. Presentations are not always linear! gnn meets llm for document-to-presentation transformation with attribution. *arXiv preprint arXiv:2405.13095*, 2024.

Tushar Aggarwal and Aarohi Bhand. Pass: Presentation automation for slide generation and speech. *arXiv preprint arXiv:2501.06497*, 2025.

Suraj Kothawade, Jiten Girdhar, Chandrashekhar Lavania, and Rishabh Iyer. Deep submodular networks for extractive data summarization. *arXiv preprint arXiv:2010.08593*, 2020.

OpenAI, Josh Achiam, Steven Adler, Sandhini Agarwal, Lama Ahmad, Ilge Akkaya, Florencia Leoni Aleman, Diogo Almeida, Janko Altenschmidt, Sam Altman, Shyamal Anadkat, Red Avila, Igor Babuschkin, Suchir Balaji, Valerie Balcom, Paul Baltescu, Haiming Bao, Mohammad Bavarian, Jeff Belgum, Irwan Bello, Jake Berdine, Gabriel Bernadett-Shapiro, Christopher Berner, Lenny Bogdonoff, Oleg Boiko, Madelaine Boyd, Anna-Luisa Brakman, Greg Brockman, Tim Brooks, Miles Brundage, Kevin Button, Trevor Cai, Rosie Campbell, Andrew Cann, Brittany Carey, Chelsea Carlson, Rory Carmichael, Brooke Chan, Che Chang, Fotis Chantzis, Derek Chen, Sully Chen, Ruby Chen, Jason Chen, Mark Chen, Ben Chess, Chester Cho, Casey Chu, Hyung Won Chung, Dave Cummings, Jeremiah Currier, Yunxing Dai, Cory Decareaux, Thomas Degry, Noah Deutsch, Damien Deville, Arka Dhar, David Dohan, Steve Dowling, Sheila Dunning, Adrien Ecoffet, Atty Eleti, Tyna Eloundou, David Farhi, Liam

Fedus, Niko Felix, Simón Posada Fishman, Juston Forte, Isabella Fulford, Leo Gao, Elie Georges, Christian Gibson, Vik Goel, Tarun Gogineni, Gabriel Goh, Rapha Gontijo-Lopes, Jonathan Gordon, Morgan Grafstein, Scott Gray, Ryan Greene, Joshua Gross, Shixiang Shane Gu, Yufei Guo, Chris Hallacy, Jesse Han, Jeff Harris, Yuchen He, Mike Heaton, Johannes Heidecke, Chris Hesse, Alan Hickey, Wade Hickey, Peter Hoeschele, Brandon Houghton, Kenny Hsu, Shengli Hu, Xin Hu, Joost Huizinga, Shantanu Jain, Shawn Jain, Joanne Jang, Angela Jiang, Roger Jiang, Haozhun Jin, Denny Jin, Shino Jomoto, Billie Jomn, Heewoo Jun, Tomer Kaftan, Łukasz Kaiser, Ali Kamali, Ingmar Kanitscheider, Nitish Shirish Keskar, Tabarak Khan, Logan Kilpatrick, Jong Wook Kim, Christina Kim, Yongjik Kim, Jan Hendrik Kirchner, Jamie Kiros, Matt Knight, Daniel Kokotajlo, Łukasz Kondraciuk, Andrew Kondrich, Aris Konstantinidis, Kyle Kosic, Gretchen Krueger, Vishal Kuo, Michael Lampe, Ikai Lan, Teddy Lee, Jan Leike, Jade Leung, Daniel Levy, Chak Ming Li, Rachel Lim, Stephanie Lin, Mateusz Litwin, Theresa Lopez, Ryan Lowe, Patricia Lue, Anna Makanju, Kim Malfacini, Sam Manning, Todor Markov, Yaniv Markovski, Bianca Martin, Katie Mayer, Andrew Mayne, Bob McGrew, Scott Mayer McKinney, Christine McLeavey, Paul McMillan, Jake McNeil, David Medina, Aalok Mehta, Jacob Menick, Luke Metz, Andrey Mishchenko, Pamela Mishkin, Vinnie Monaco, Evan Morikawa, Daniel Mossing, Tong Mu, Mira Murati, Oleg Murk, David Mély, Ashvin Nair, Reiichiro Nakano, Rajeev Nayak, Arvind Neelakantan, Richard Ngo, Hyeonwoo Noh, Long Ouyang, Cullen O’Keefe, Jakub Pachocki, Alex Paino, Joe Palermo, Ashley Pantuliano, Giambattista Parascandolo, Joel Parish, Emy Parparita, Alex Passos, Mikhail Pavlov, Andrew Peng, Adam Perelman, Filipe de Avila Belbute Peres, Michael Petrov, Henrique Ponde de Oliveira Pinto, Michael, Pokorny, Michelle Pokrass, Vitchyr H. Pong, Tolly Powell, Alethea Power, Boris Power, Elizabeth Proehl, Raul Puri, Alec Radford, Jack Rae, Aditya Ramesh, Cameron Raymond, Francis Real, Kendra Rimbach, Carl Ross, Bob Rotstet, Henri Roussez, Nick Ryder, Mario Saltarelli, Ted Sanders, Shibani Santurkar, Girish Sastry, Heather Schmidt, David Schnurr, John Schulman, Daniel Selsam, Kyla Sheppard, Toki Sherbakov, Jessica Shieh, Sarah Shoker, Pranav Shyam, Szymon Sidor, Eric Sigler, Maddie Simens, Jordan Sitkin, Katarina Slama, Ian Sohl, Benjamin Sokolowsky, Yang Song, Natalie Staudacher, Felipe Petroski Such, Natalie Summers, Ilya Sutskever, Jie Tang, Nikolas Tezak, Madeleine B. Thompson, Phil Tillet, Amin Tootoonchian, Elizabeth Tseng, Preston Tuggle, Nick Turley, Jerry Tworek, Juan Felipe Cerón Uribe, Andrea Vallone, Arun Vijayvergiya, Chelsea Voss, Carroll Wainwright, Justin Jay Wang, Alvin Wang, Ben Wang, Jonathan Ward, Jason Wei, CJ Weinmann, Akila Welihinda, Peter Welinder, Jiayi Weng, Lilian Weng, Matt Wiethoff, Dave Willner, Clemens Winter, Samuel Wolrich, Hannah Wong, Lauren Workman, Sherwin Wu, Jeff Wu, Michael Wu, Kai Xiao, Tao Xu, Sarah Yoo, Kevin Yu, Qiming Yuan, Wojciech Zaremba, Rowan Zellers, Chong Zhang, Marvin Zhang, Shengjia Zhao, Tianhao Zheng, Juntang Zhuang, William Zhuk, and Barret Zoph. Gpt-4 technical report, 2024. URL <https://arxiv.org/abs/2303.08774>.

Zhilin Zhang, Xiang Zhang, Jiaqi Wei, Yiwei Xu, and Chenyu You. Postergen: Aesthetic-aware paper-to-poster generation via multi-agent llms. *arXiv preprint arXiv:2508.17188*, 2025d.

Xiang Zhang, Bradley Hauer, and Grzegorz Kondrak. Improving hownet-based chinese word sense disambiguation with translations. In *Findings of the Association for Computational Linguistics: EMNLP 2022*, pages 4530–4536, 2022.

Jiaqi Wei, Xiang Zhang, Yuejin Yang, Wenxuan Huang, Juntai Cao, Sheng Xu, Xiang Zhuang, Zhangyang Gao, Muhammad Abdul-Mageed, Laks VS Lakshmanan, et al. Unifying tree search algorithm and reward design for llm reasoning: A survey. *arXiv preprint arXiv:2510.09988*, 2025a.

Humza Naveed, Asad Ullah Khan, Shi Qiu, Muhammad Saqib, Saeed Anwar, Muhammad Usman, Naveed Akhtar, Nick Barnes, and Ajmal Mian. A comprehensive overview of large language models. *ACM Transactions on Intelligent Systems and Technology*, 16:1–72, 2025.

Jiaqi Wei, Yuejin Yang, Xiang Zhang, Yuhan Chen, Xiang Zhuang, Zhangyang Gao, Dongzhan Zhou, Guangshuai Wang, Zhiqiang Gao, Juntai Cao, et al. From ai for science to agentic science: A survey on autonomous scientific discovery. *arXiv preprint arXiv:2508.14111*, 2025b.

Chin-Yew Lin. Rouge: A package for automatic evaluation of summaries. In *Text summarization branches out*, pages 74–81, 2004.

Fred Jelinek, Robert L Mercer, Lalit R Bahl, and James K Baker. Perplexity—a measure of the difficulty of speech recognition tasks. *The Journal of the Acoustical Society of America*, 62(S1):S63–S63, 1977.

Xiang Zhang, Senyu Li, Bradley Hauer, Ning Shi, and Grzegorz Kondrak. Don’t trust chatgpt when your question is not in english: a study of multilingual abilities and types of llms. *arXiv preprint arXiv:2305.16339*, 2023.

Li Sun, Liu He, Shuyue Jia, Yangfan He, and Chenyu You. Docagent: An agentic framework for multi-modal long-context document understanding. In *Proceedings of the Conference on Empirical Methods in Natural Language Processing*, pages 17712–17727, 2025.

Table of Contents

| | |
|---|----|
| Section A: Data and Evaluation | 1 |
| A.1. Dataset | 1 |
| A.2. Notation | 3 |
| A.3. Geometry-Aware Density | 3 |
| A.4. SlideQA Protocol | 5 |
| A.5. Perplexity (PPL) | 6 |
| Section B: Additional Analysis | 6 |
| B.1. Efficiency and Cost | 6 |
| B.2. Backbone-Specific Prompt Structure Sensitivity | 7 |
| B.3. User Study | 8 |
| B.4. Dataset Scope and Generalizability | 9 |
| Section C: Abbreviations | 9 |
| Section D: Samples Generated by Our Pipeline | 10 |
| Section E: Samples Generated by Baselines | 12 |
| Section F: Template Library | 12 |
| Section G: Prompts | 12 |
| Section H: Example Outputs from Agents | 12 |
| Section I: Color Setting | 15 |

Fei Xiong, Xiang Zhang, Aosong Feng, Siqi Sun, and Chenyu You. Quantagent: Price-driven multi-agent llms for high-frequency trading. *arXiv preprint arXiv:2509.09995*, 2025.

Chenyu You, Haocheng Dai, Yifei Min, Jasjeet S Sekhon, Sarang Joshi, and James S Duncan. Uncovering memorization effect in the presence of spurious correlations. *Nature Communications*, 16(1):5424, 2025.

Bo Li, Yuanhan Zhang, Dong Guo, Renrui Zhang, Feng Li, Hao Zhang, Kaichen Zhang, Yanwei Li, Ziwei Liu, and Chunyuan Li. Llava-onevision: Easy visual task transfer, 2024. URL <https://arxiv.org/abs/2408.03326>.

Peng Wang, Shuai Bai, Sinan Tan, Shijie Wang, Zhihao Fan, Jinze Bai, Keqin Chen, Xuejing Liu, Jialin Wang, Wenbin Ge, Yang Fan, Kai Dang, Mengfei Du, Xuancheng Ren, Rui Men, Dayiheng Liu, Chang Zhou, Jingren Zhou, and Junyang Lin. Qwen2-vl: Enhancing vision-language model’s perception of the world at any resolution. *arXiv preprint arXiv:2409.12191*, 2024.

Jinze Bai, Shuai Bai, Shusheng Yang, Shijie Wang, Sinan Tan, Peng Wang, Junyang Lin, Chang Zhou, and Jingren Zhou. Qwen-vl: A versatile vision-language model for understanding, localization, text reading, and beyond. *arXiv preprint arXiv:2308.12966*, 2023.

Qwen Team. Qwen2.5-vl, January 2025. URL <https://qwenlm.github.io/blog/qwen2.5-vl/>.

Abdelrahman Abouelenin, Atabak Ashfaq, Adam Atkinson, Hany Awadalla, Nguyen Bach, Jianmin Bao, Alon Ben-haim, Martin Cai, Vishrav Chaudhary, Congcong Chen, et al. Phi-4-mini technical report: Compact yet powerful multimodal language models via mixture-of-loras. *arXiv preprint arXiv:2503.01743*, 2025.

A Data and Evaluation

A.1 Dataset

We include 200 peer-reviewed papers from leading AI venues between 2022 and 2025. Table 6 reports counts by venue and year. The selected conferences were chosen for their rigorous review process, topical breadth, including multimodal learning, generative modeling, interpretability, and frequent inclusion of rich visual and mathematical content, making them ideal for downstream tasks such as slide generation, summarization, and modality-aware learning.

Table 3 Comprehensive comparison of automatic slide generation systems. The table summarizes key capabilities of existing approaches. **SlideGen** is the first unified framework that fulfills all major functional criteria, integrating complete content planning, layout reasoning, and visual refinement. **Columns:** *Content Struct.* – whether the system constructs a slide-level outline; *Text–Fig Align.* – alignment of figures and tables with corresponding text; *Multimodal* – support for inputs beyond text; *Output Format* – type of generated presentation file; *Pref. Eval.* – automatic evaluation via trained preference models (e.g., PREVAL, PPTEval); *Iter. Visual Opt.* – post-render refinement of visual layout; *Fine Layout Ctrl.* – explicit element placement using coordinates or bounding boxes; *Aesthetic Priors* – design priors learned from expert-authored slides; *User Editability* – support for designers to easily modify or extend the output before generating the final PPT file (e.g., iterative user input loops or configurable parameters). **Legend:** ✓ = supported; ○ = partly supported; ✗ = not supported. See Table 4 for the per-column scoring legend.

| Framework | Content Struct. | Text–Fig Align. | Multi Modal | Output Format | Pref. Eval. | Iter. Visual Opt. | Fine Layout Ctrl. | Aesthetic Priors | User Editability |
|--|-----------------|-----------------|-------------|---------------|-------------|-------------------|-------------------|------------------|------------------|
| PPSGen (2013) (Hu and Wan, 2013) | ○ | ✗ | ✗ | text | ✗ | ✗ | ✗ | ✗ | ✗ |
| D2S (2021) (Sun et al., 2021) | ○ | ✓ | ✓ | text | ✗ | ✗ | ✗ | ✗ | ✗ |
| DOC2PPT (2022) (Fu et al., 2022) | ✓ | ✓ | ✓ | PPTX/PDF | ✗ | ✗ | ✓ | ✓ | ✗ |
| Persona-Aware D2S (2024) (Mondal et al., 2024) | ✓ | ○ | ✓ | PDF | ✗ | ✗ | ✗ | ✗ | ✗ |
| GDP (2024) (Maheshwari et al., 2024) | ✓ | ✗ | ✗ | text | ✗ | ✗ | ✗ | ✗ | ✗ |
| DocPres (2024) (Bandyopadhyay et al., 2024) | ✓ | ○ | ✓ | PDF | ✗ | ✗ | ○ | ✗ | ✗ |
| PASS (2025) (Aggarwal and Bhand, 2025) | ✓ | ○ | ✓ | PPTX | ✗ | ✗ | ✗ | ✗ | ✗ |
| RCPS (2025) (Xi et al., 2025) | ✓ | ✓ | ✓ | PPTX/PDF | ✓ | ✓ | ✓ | ○ | ✗ |
| PPTAgent (2025) (Zheng et al., 2025) | ✓ | ✓ | ✓ | PPTX/HTML | ✓ | ✓ | ○ | ○ | ✓ |
| Auto-Slides (2025) (Yang et al., 2025) | ✓ | ✓ | ✓ | PDF | ✗ | ✓ | ○ | ○ | ✗ |
| AutoPresent (2025) (Ge et al., 2025) | ✗ | ○ | ✓ | PPTX | ✓ | ✓ | ✓ | ○ | ✗ |
| SlideGen (Ours) | ✓ | ✓ | ✓ | PPTX | ✓ | ✓ | ✓ | ✓ | ✓ |

Table 4 Per-column scoring legend for ✓ / ○ / ✗.

| Column | ✓ (supported) | ○ (partly) | ✗ (not) |
|--------------------------|---|---------------------------------------|---|
| Content Struct. | Clear slide-level outline (sections → slides → key points). | Topic list only. | No outline. |
| Text–Fig Align. | Precise pairing with explicit loss or post-process. | Heuristic or example-based placement. | Not handled. |
| Multi Modal | Text + images (optionally formulas/audio). | Partial multimodality. | Text only. |
| Pref. Eval. | Trained preference model (e.g., PREVAL/PPTEval). | LLM heuristic scoring only. | ROUGE or human-only. |
| Iter. Visual Opt. | Multi-round render-critique-revise. | Single-pass minor refine. | One-shot generation. |
| Fine Layout Ctrl. | BBox/coordinates or constraints. | Coarse slots/templates. | None. |
| Aesthetic Priors | Learns from high-quality slides (imitation/distillation). | Weak/indirect prior. | None. |
| User Editability | Supports pre-generation modifications (e.g., user feedback loops, customizable templates/parameters). | - | No user intervention before final output. |

A.2 Notation

A deck consists of N slides $\{s_i\}_{i=1}^N$. Each slide has a role $r_i \in \{\text{title}, \text{agenda}, \text{content}, \text{thanks}\}$. For **content** slides we record an optional *section* label $\sigma_i \in \Sigma$ and *subsection* label $\sigma'_i \in \Sigma'$. We denote the pattern identifier by $\pi_i \in \mathcal{P}$ (e.g., **T1_TextOnly**, **T4_ImageTop**).

We consider a fixed slide layout: slide s_1 is the **title** page, slide s_2 is the **agenda** page, slides s_3, \dots, s_{N-1} are **content** pages, and the last slide s_N is **thanks** page. Formally, a deck has N slides $\{s_i\}_{i=1}^N$ with roles $r_1 = \text{title}$, $r_2 = \text{agenda}$, $r_i = \text{content}$ for $3 \leq i \leq N-1$, and $r_N = \text{thanks}$. The content page lists *section dividers* (“PART 1, PART 2, …”); these are the *agenda items*. Let $\mathcal{A} = [a_1, \dots, a_m]$ be the ordered list of top-level bullets on s_2 .

Each slide carries a hierarchical string bullet list B_i , where each content box b is defined as a pair $(u_{i,k}, \mathcal{S}_{i,k})$, and $u_{i,k}$ is the k -th top-level bullet.

Image, table, and formula assets on slide i are denoted by the finite sets \mathcal{I}_i for image filenames, \mathcal{T}_i for table filenames, and \mathcal{F}_i for LaTeX strings, respectively. Optional speaker notes are written n_i . Let slide area be 1. For each region $b \in \mathcal{B}_i$ with normalized width and height w_b, h_b . The occupied area is the union area $\rho_i \in [0, 1]$ of all non-background regions.

A.3 Geometry-Aware Density

This metric evaluates layout density with two components: (i) area occupancy relative to a target τ ; (ii) a concave quadratic preference over the effective number of content boxes, peaking at M^* .

Why a downward-opening scoring function? Overly monolithic slides look blocky and lack hierarchy, while excessive partitioning introduces noise and jumpy reading. A downward-opening scoring function over the effective region count captures the optimal range: it peaks near the preferred count M^* , then smoothly decreases as the count drifts left, where pages become too plain, or right, where they become too busy, avoiding brittle thresholds. The width κ controls tolerance around M^* , and the area gate a_{\min} prevents gaming with tiny micro-regions. Combined with the occupancy term $1 - |\rho_i - \tau|$, this yields an interpretable and reproducible measure that rewards layouts which are neither sparse nor cluttered.

We count only non-trivial regions via a minimum area gate $a_{\min} > 0$:

$$M_i^{\text{eff}} = \sum_{b \in \mathcal{B}_i} \mathbf{1}[A(b) \geq a_{\min}]. \quad (\text{A.1})$$

Define a downward-opening quadratic fragmentation reward with maximum at M^* :

$$R_i^{\text{frag}} = \max \left\{ 0, 1 - \frac{(M_i^{\text{eff}} - M^*)^2}{\kappa} \right\} \in [0, 1]. \quad (\text{A.2})$$

$$\text{OM}_i \triangleq 1 - |\rho_i - \tau|, \quad \text{FR}_i \triangleq R_i^{\text{frag}}. \quad (\text{A.3})$$

$$s_i^{\text{geom}} = \lambda_1 \text{OM}_i + \lambda_2 \text{FR}_i, \quad \lambda_1 + \lambda_2 = 1, \quad (\text{A.4})$$

$$\text{DENSITY}^{\text{geom}} = \frac{1}{N} \sum_{i=1}^N (\lambda_1 \text{OM}_i + \lambda_2 \text{FR}_i). \quad (\text{A.5})$$

We set $a_{\min} = 0.04$, $\tau = 0.55$. The weights λ_1 and λ_2 are determined based on the values of b_1 and b_2 , which are introduced later in the text. Specifically, we set:

$$\lambda_1 = \frac{b_1}{b_1 + b_2}, \quad \lambda_2 = \frac{b_2}{b_1 + b_2}. \quad (\text{A.6})$$

This ensures that the sum of λ_1 and λ_2 equals 1, while λ_1 and λ_2 are proportional to b_1 and b_2 , respectively.

Algorithm 1: LODO training and prediction with linear regression mapping (OM/FR \rightarrow human score)

Input : Dataset $\mathcal{D} = \{(deck_i, page_i, y_i, \rho_i, M_i^{\text{eff}})\}_{i=1}^N$; fixed a_{\min}, τ ; grid $M^* \in [m_{\min}, m_{\max}]$, $\kappa \in [\kappa_{\min}, \kappa_{\max}]$ with step $\Delta\kappa$

Output : Per-fold params $\{M_d^*, \kappa_d, a_d, b_{1,d}, b_{2,d}\}$; predictions $\{\hat{y}^{\text{raw}}, \hat{y}^{[1,5]}\}$

Initialize prediction list $\mathcal{P} \leftarrow \emptyset$ and parameter table $\Theta \leftarrow \emptyset$

for each deck d do

$\mathcal{D}_{\text{train}} \leftarrow \{i : \text{deck}_i \neq d\}$, $\mathcal{D}_{\text{val}} \leftarrow \{i : \text{deck}_i = d\}$ // leave-one-deck-out

$(M_d^*, \kappa_d, a_d, b_{1,d}, b_{2,d}) \leftarrow \text{SELECTANDFIT}(\mathcal{D}_{\text{train}}, \tau, [m_{\min}, m_{\max}], [\kappa_{\min}, \kappa_{\max}], \Delta\kappa)$ // see Algorithm 2 for details

for each $i \in \mathcal{D}_{\text{val}}$ do

$\text{OM}_i \leftarrow 1 - |\rho_i - \tau|$

$\text{FR}_i \leftarrow \max\left(0, 1 - \frac{(M_i^{\text{eff}} - M_d^*)^2}{\kappa_d}\right)$

$\hat{y}_i^{\text{raw}} \leftarrow a_d + b_{1,d} \text{OM}_i + b_{2,d} \text{FR}_i$

$\hat{y}_i^{[1,5]} \leftarrow \text{clip}(\hat{y}_i^{\text{raw}}, 1, 5)$

Append $(\text{deck}_i, \text{page}_i, y_i, \hat{y}_i^{\text{raw}}, \hat{y}_i^{[1,5]})$ to \mathcal{P}

Record $(d, M_d^*, \kappa_d, a_d, b_{1,d}, b_{2,d})$ into Θ

Compute overall Pearson/Spearman using \hat{y}^{raw} and RMSE using $\hat{y}^{[1,5]}$

return Θ and \mathcal{P}

Algorithm 2: SelectAndFit

Input : train_idx, tau, m_min, m_max, kappa_min, kappa_max, delta_kappa

Output : best_M, best_kappa, a, b1, b2

Extract y[i], rho[i], Meff[i] for i in train_idx

foreach i in train_idx **do**

$\text{OM}[i] \leftarrow 1 - \text{abs}(\text{rho}[i] - \tau)$

best_key $\leftarrow (-\text{INF}, -\text{INF}, +\text{INF})$

$(\text{best_M}, \text{best_kappa}, \text{a}, \text{b1}, \text{b2}) \leftarrow (0, 0, 0, 0, 0)$

for $M_{\text{star}} \leftarrow m_{\min} m_{\max}$ **do**

for $\kappa \leftarrow \kappa_{\min}; \kappa \leq \kappa_{\max}; \kappa \leftarrow \kappa + \Delta\kappa$ **do**

foreach i in train_idx **do**

$\text{FR}[i] \leftarrow \max(0, 1 - ((\text{Meff}[i] - M_{\text{star}})^2) / (\kappa))$

$(\text{a}, \text{b1}, \text{b2}) \leftarrow \text{LinearLeastSquares}(\text{y}, [1, \text{OM}, \text{FR}])$

for i in train_idx **do**

$\text{y_raw}[i] \leftarrow \text{a} + \text{b1} * \text{OM}[i] + \text{b2} * \text{FR}[i]$

$\text{y_clip}[i] \leftarrow \text{clip}(\text{y_raw}[i], 1, 5)$

// Evaluate

$\text{pearson} \leftarrow \text{Pearson}(\text{y}, \text{y_raw})$

$\text{spearman} \leftarrow \text{Spearman}(\text{y}, \text{y_raw})$

$\text{rmse} \leftarrow \text{RMSE}(\text{y}, \text{y_clip})$

$\text{key} \leftarrow (\text{pearson}, \text{spearman}, -\text{rmse})$

if $\text{key} > \text{best_key}$ **then**

$\text{best_key} \leftarrow \text{key}$

$(\text{best_M}, \text{best_kappa}, \text{a}, \text{b1}, \text{b2}) \leftarrow (M_{\text{star}}, \kappa, \text{a}, \text{b1}, \text{b2})$

return $(\text{best_M}, \text{best_kappa}, \text{a}, \text{b1}, \text{b2})$

Table 5 PPTEVAL dimensions and criteria (1–5 scale), adapted from (Zheng et al., 2025).

| Dimension | Criteria |
|------------------|---|
| Content | Text is concise and grammatically sound; key points are supported by relevant images. |
| Design | Harmonious colors and proper layout ensure readability; visual elements enhance appeal without clutter. |
| Coherence | Structure progresses logically and includes essential background information across the deck. |

A.3.1 Training Method

Data and preprocessing. For each deck d and page i we parse a JSON file that provides the page size, and the sizes, positions, and raw text content of content boxes \mathcal{B}_i . Human judgments were obtained from $R = 40$ recruited raters. Raters score each slide on a 1-5 scale (to one decimal place, in 0.1 increments): **1** = extremely cluttered or extremely sparse; **3** = broadly acceptable but not ideal; **5** = very clean with appropriate information density. To remove differences in how strict or easy each rater scores, we perform per-rater z -score normalization:

$$z_{d,i}^{(r)} = \frac{s_{d,i}^{(r)} - \mu_r}{\sigma_r + \varepsilon}, \quad \mu_r = \text{mean}_{d,i}[s_{d,i}^{(r)}], \quad \sigma_r = \text{std}_{d,i}[s_{d,i}^{(r)}]. \quad (\text{A.7})$$

Density score and human score mapping. Instead of a manually set weighted sum, we learn an affine mapping from geometry score to the human scale:

$$\hat{y}_{d,i} = a + b_1 \text{OM}_{d,i} + b_2 \text{FR}_{d,i}, \quad (\text{A.8})$$

with (a, b_1, b_2) fit by least squares on training pages.

Grid search over (M^*, κ) . We select (M^*, κ) by a grid $M^* \in \{m_{\min}, \dots, m_{\max}\}$ and $\kappa \in \{\kappa_{\min}, \kappa_{\min} + \Delta, \dots, \kappa_{\max}\}$, as shown in Figure 9(c). For each grid point we recompute FR, refit (a, b_1, b_2) by least squares on the training split, and evaluate: (i) Pearson’s r on \hat{y} ; (ii) Spearman’s ρ on \hat{y} ; (iii) RMSE on $\text{clip}(\hat{y}, 1, 5)$.

Cross-deck evaluation. To assess generalization to unseen decks, we adopt Leave-One-Deck-Out cross-validation. For each validation deck d^{val} :

1. Train on $\mathcal{D} \setminus \{d^{\text{val}}\}$: run the grid search to select (M^*, κ) and fit (a, b_1, b_2) by least squares.
2. Validate on d^{val} : compute (OM, FR) and predict \hat{y} using the learned parameters.

We concatenate predictions across folds and report global Pearson and Spearman on \hat{y} , and RMSE on clipped \hat{y} .

Implementation notes. We keep a_{\min} and τ fixed, only (M^*, κ) are selected per fold by the grid, while (a, b_1, b_2) are re-fit by least squares, see Algorithm 1 for training details. Per-rater z -score aggregation reduces rater bias and stabilizes the target scale. Section pages (e.g., “PART 01”) are filtered before feature extraction and learning.

A.4 SlideQA Protocol

The protocol of SlideQA is as follows: **(i) Question curation:** For each source paper, we follow a deck-reader communication setup (Pang et al., 2025) and employ ChatGPT-4o as a question-generation model to produce $|\mathcal{Q}_{\text{eval}}| = 100$ multiple-choice questions per paper. We construct two disjoint subsets: $\mathcal{Q}_{\text{verb}}$ with $|\mathcal{Q}_{\text{verb}}| = 50$ *verbatim* questions directly answerable from the paper text, spanning 13 content aspects; and \mathcal{Q}_{int} with $|\mathcal{Q}_{\text{int}}| = 50$ *interpretive* questions targeting high-level comprehension across 10 conceptual dimensions. We set $\mathcal{Q}_{\text{eval}} = \mathcal{Q}_{\text{verb}} \cup \mathcal{Q}_{\text{int}}$ and $\mathcal{Q}_{\text{verb}} \cap \mathcal{Q}_{\text{int}} = \emptyset$. **(ii) Respondents:** Each image is presented to $M = 6$ vision-language models, a mix of open- and closed-source systems, including three closed-source models: GPT-4o-mini, GPT-4o, and GPT-o3, and three open-source models: LLaVA-OV-7B, Qwen2.5-VL-7B-Instruct, and Phi-4-multimodal-instruct, to simulate reader standards from casual to expert (Pang et al.,

Table 6 Number of papers by Conference and Year

| Conference | 2022 | 2023 | 2024 | 2025 |
|------------|------|------|------|------|
| ICLR | 17 | 31 | 29 | 23 |
| ICML | — | 16 | 24 | 30 |
| NeurIPS | — | 10 | 20 | — |

2025). The abilities of closed-source vision-language models typically surpass those of open-source models, similar to higher-performing students achieving better exam scores. To make the reading setting both fair and realistic, we provide each model with the full slide deck, including both the rendered slides and the speaker notes produced by our Speaker Agent. Models must answer all questions based solely on this combined content. We report accuracy rate as our evaluation metric. The exact question-generation prompt is shown in Figures 28, 29, 30, 31.

Definition. Let $r_{q,m} \in \{0,1\}$ denote the correctness of model $m \in \{1, \dots, M\}$ on question $q \in \mathcal{Q}_{\text{eval}}$. Define the per-question averaged correctness

$$\bar{r}_q = \frac{1}{M} \sum_{m=1}^M r_{q,m}. \quad (\text{A.9})$$

The SlideQA accuracy is then

$$s_R = \frac{1}{|\mathcal{Q}_{\text{eval}}|} \sum_{q \in \mathcal{Q}_{\text{eval}}} \bar{r}_q, \quad (\text{A.10})$$

which averages correctness across both questions and models. Subset scores restrict the sum in equation A.10 to $\mathcal{Q}_{\text{verb}}$ and \mathcal{Q}_{int} :

$$s_R^{\text{verb}} = \frac{1}{|\mathcal{Q}_{\text{verb}}|} \sum_{q \in \mathcal{Q}_{\text{verb}}} \bar{r}_q, \quad s_R^{\text{int}} = \frac{1}{|\mathcal{Q}_{\text{int}}|} \sum_{q \in \mathcal{Q}_{\text{int}}} \bar{r}_q. \quad (\text{A.11})$$

Rationale. This protocol simulates how readers gain information from slides: questions come from the paper, but answers must be inferred solely from the slides.

A.5 Perplexity (PPL)

What it measures. It quantifies the average next-token uncertainty of a language model over the deck text. Lower values indicate more fluent and predictable text. We compute this metric using Llama-2-7b-hf language model.

Definition. Let $T(\cdot)$ be a fixed tokenizer and let

$$x_{1:L} = T(\text{flat}(B_1) \parallel \dots \parallel \text{flat}(B_N))$$

be the token sequence obtained by concatenating all slide texts. The full-sequence perplexity is

$$\text{PPL} = \exp\left(-\frac{1}{L} \sum_{t=1}^L \log p_{\theta}(x_t \mid x_{<t})\right), \quad (\text{A.12})$$

where \log denotes the natural logarithm. Lower PPL means higher predicted likelihood per token, $\text{PPL} = 1$ corresponds to perfectly predictable text.

B Additional Analysis

B.1 Efficiency and Cost

All runs use the same prompts, template set, and decoding settings on the same machine.

We aggregate by variant and agent over the full test set. Total time equals the sum of wall-clock seconds. Total tokens equal input plus output tokens. Cost (USD) is computed with per-1K token pricing for input and output:

$$\text{Cost} = \frac{\text{input_tokens}}{1000} C_{\text{in}} + \frac{\text{output_tokens}}{1000} C_{\text{out}}. \quad (\text{B.1})$$

We visualize three horizontal stacked bar charts. Each bar corresponds to a model variant. Figure 11 shows per-agent contributions for (a) time, (b) tokens, and (c) cost.

B.2 Backbone-Specific Prompt Structure Sensitivity

In this section, we analyze the sensitivity of model performance to the structure of the prompts, specifically focusing on the system prompt and output structure. We hypothesize that for models like GPT-5, the structure of the prompt, rather than the task complexity, plays a significant role in output alignment and content richness. This experiment investigates how different prompt structures affect the ability of models to generate well-formed, format-compliant outputs and how detailed the generated content is. We specifically evaluate two prompt structures across three models: GPT-4o, GPT-5, and Qwen2.5-VL-7B.

Experimental Setup. We evaluate two types of prompt structures: (i) **System-Long**: The system prompt includes both the high-level task description and detailed instructions for output formatting, including format constraints (such as JSON schema) and example outputs. (ii) **System-Minimal + Template-Based Output**: The system prompt is limited to a single sentence outlining the task’s objective, with detailed formatting instructions, JSON schema, and example outputs moved into a separate template block.

The experiment involves two tasks within the SlideGen pipeline: Outliner and Arranger. In each case, the system prompt is altered according to the two prompt structures, while the input paper and model settings remain fixed.

Metrics. We assess the performance of each model with the following key metrics: (i) **Output Alignment** (\uparrow): The proportion of outputs that strictly adhere to the required format constraints (such as the JSON schema). Higher output alignment indicates better compliance with the specified output structure. (ii) **Content Richness** (\uparrow): This metric measures the richness of the generated content by counting the number of JSON "lines" (bullet points and fields). We normalize the richness by using model-specific baselines: For GPT-5, 600 lines = 100; For GPT-4o and Qwen, 250 lines = 100.

Higher content richness indicates a more detailed output, with more sections and subsections generated by the model.

Results. Figure 10 presents the experimental results, showing how the two prompt structures (System-Long vs. System-Minimal+Template-Based Output) affect the performance of GPT-4o, GPT-5, and Qwen across Speaker and Arranger tasks in terms of Content Richness.

Analysis. The results clearly demonstrate that the System-Minimal + Template-Based Output structure significantly improves GPT-5’s content richness, generating more detailed and comprehensive outputs, compared to the System-Long structure. In particular, GPT-5, under the System-Long structure, generates less detailed content, with fewer sections and subsections, leading to a lower content richness score. However, when using System-Minimal + Template-Based Output, GPT-5’s content richness increases significantly, reflecting more detailed output and greater structural depth.

In contrast, GPT-4o shows stable performance across both prompt structures, with high content richness regardless of the structure. This suggests that GPT-4o is less sensitive to prompt structure and can generate detailed content even under the simpler System-Long structure.

Qwen2.5-VL-7B, while showing some improvement with the System-Minimal + Template-Based Output structure, still lags behind both GPT-4o and GPT-5 in content richness.

Conclusion. This experiment validates that for models like GPT-5, prompt structure plays a crucial role in ensuring content richness. By keeping the system prompt minimal and moving instructions and output structure into the template block, we can significantly improve GPT-5’s performance in generating detailed

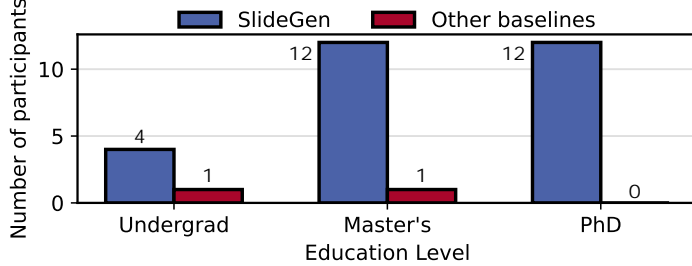


Figure 12 The preference distribution of participants across different education levels for the slide deck generation task.

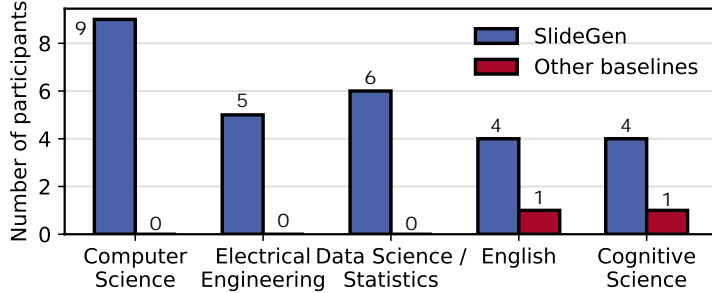


Figure 13 The preference distribution of participants across different majors.

and structured outputs. While GPT-4o remains relatively insensitive to prompt structure, the improvements observed with GPT-5 demonstrate the importance of careful prompt design in ensuring model alignment to task-specific formats. Future work could explore similar prompt structures for other tasks and models to further enhance the robustness and flexibility of the pipeline.

B.3 User Study

As illustrated in Figure 13, we surveyed participants from various academic majors to assess how their preferences for SlideGen-generated slide decks varied. The figure depicts the preference distribution across five key fields: Computer Science, Electrical Engineering, Data Science/Statistics, English, and Cognitive Science.

To evaluate the practical utility and perceived quality of our generated presentations, we conducted a user study with 30 participants from our target demographic—graduate students and researchers with prior experience in preparing and delivering academic presentations. Participants reviewed 10 randomly selected PPTX slide decks generated by SlideGen and competing baselines. As shown in Figure 12, the participant pool included 4 undergraduate students, 14 master’s students, and 12 PhD students. The figure highlights preference distributions by education level, with most participants favoring SlideGen-generated decks, particularly those from master’s and PhD backgrounds.

Table 7 presents the highly encouraging results from this user study. Participants responded to two key questions regarding their preferences and the perceived quality of SlideGen-generated slide decks.

In response to Q1 ("Which slide deck would you choose as your presentation draft?"), an overwhelming 93.33% selected the SlideGen-generated deck, compared to just 6.67% for other baselines. For Q2 ("How does SlideGen’s output compare to human-made slides?"), 73.33% rated it as "better than most humans," and 6.67% deemed it "top-tier, expert quality." Notably, none rated it as "worse than most humans."

Overall, the results indicate a strong preference for SlideGen-generated decks, with the highest endorsement from participants in Data Science/Statistics and Computer Science. Even among those in English and Cognitive Science, a notable portion expressed approval, underscoring SlideGen’s broad appeal across academic disciplines.

Table 7 User Study Results. We surveyed target users to evaluate SlideGen’s utility and quality. The table shows responses to two key questions.

| Question | Response Option | Distribution |
|--|---------------------------------------|---------------|
| Q1: Which slide deck would you choose as your presentation draft? | Our Method (SlideGen) | 93.33% |
| | Other Baselines | 6.67% |
| Q2: How does SlideGen’s output compare to human-made slides? | A. Worse than most humans | 0% |
| | B. about as good as an average person | 20.00% |
| | C. Better than most humans | 73.33% |
| | D. Top-tier, expert quality | 6.67% |

B.4 Dataset Scope and Generalizability

In this work, we constructed our dataset primarily from Computer Science (CS) research papers published in top-tier Artificial Intelligence (AI) conferences. This focused approach was a deliberate design choice for two key reasons:

1. **Domain Expertise and Evaluation Feasibility:** Our expertise in the AI field was essential for accurately evaluating the quality and logical coherence of the generated slides during framework development.
2. **Focus on Scientific Communication:** Our framework targets the common structure of scientific papers (e.g., Intro, Methods, Results). While our dataset is from CS, the methodology is inherently domain-agnostic across scientific fields like medicine, physics, and biology.

Generalizability to Broader Domains. Beyond academic papers, we believe our core framework is highly extensible to other domains, such as business reports, legal documents, or even creative fields like art and photography. The primary adaptation required would be the expansion of the template library.

For instance, applying our framework to the art domain would involve curating a set of presentation templates that are visually suited for showcasing artwork (e.g., more image-centric layouts, different font styles, and color palettes). This task of template creation and curation does not require fundamental changes to our core framework and can be accomplished by designers. This modularity is a key strength of our approach, allowing it to be readily adapted to new domains by simply swapping or expanding the design templates.

In summary, while we focus on CS for rigorous validation, our methodology is broadly applicable across domains.

C Abbreviations

We provide a reference for the abbreviations of models used in this paper, as show in Table 8.

Table 8 Reference for model abbreviations used in this paper.

| Abbreviation | Full Name |
|----------------|---|
| 4o-mini | GPT-4o-mini |
| 4o | GPT-4o |
| o3 | GPT-o3 |
| llava-ov-7b | LLaVA-OneVision-Qwen2-7b-ov-hf (Li et al., 2024) |
| Qwen2.5-VL-7B | Qwen2.5-VL-7B-Instruct (Wang et al., 2024; Bai et al., 2023) |
| Qwen2.5-VL-72B | Qwen2.5-VL-72B-Instruct (Wang et al., 2024; Bai et al., 2023; Team, 2025) |
| Phi-4-MM | Phi-4-multimodal-instruct (Abouelenin et al., 2025) |

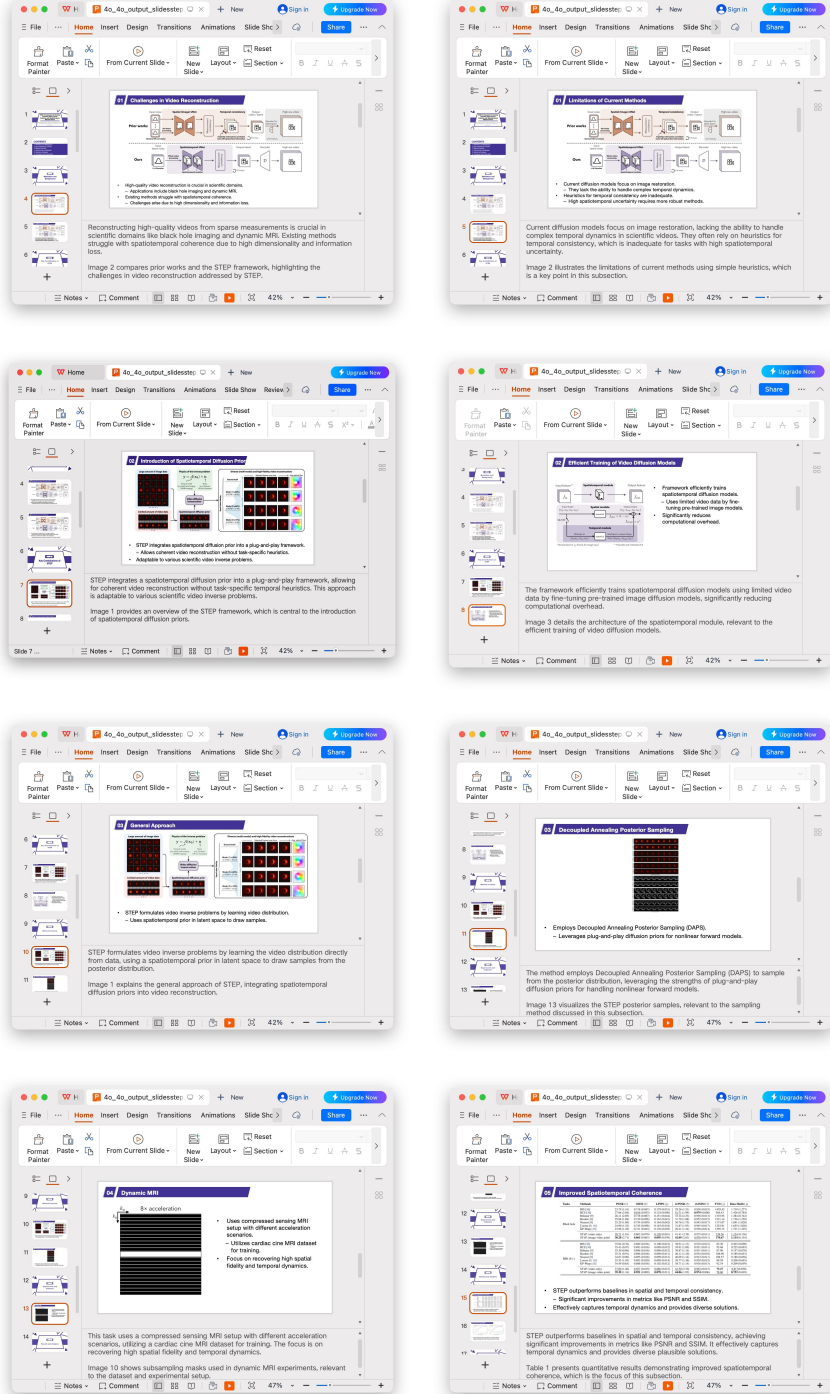


Figure 14 Generated notes. The figure shows screenshots of SlideGen-generated slides as viewed within WPS.

D Samples Generated by Our Pipeline

Below are samples generated by our method default deep blue color as theme color on the Paper2Slide task: Figures 15, 16, 17, 18, and 19.

Figures 20, 21, and 22 show examples where the paper's colors are extracted and refined by the Color Refiner

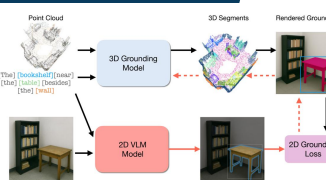
From Thousands to Billions: 3D Visual Language Grounding via Render-Supervised Distillation from 2D VLMs

Ang Cao, Sergio Arnaud, Oleksandr Maksymets,
Jianing Yang, Ayush Jain, Ada Martin, Vincent-Pierre Berges, Paul McVay, Ruslan Partsey...

CONTENTS

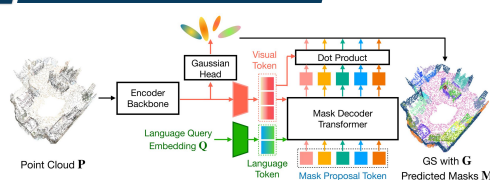
- 1. Motivation and Background
- 2. Key Contributions
- 3. Method Overview
- 4. Experiments and Datasets
- 5. Results and Analysis
- 6. Conclusion and Future Work

01 The Data Scarcity Challenge in 3D VLG



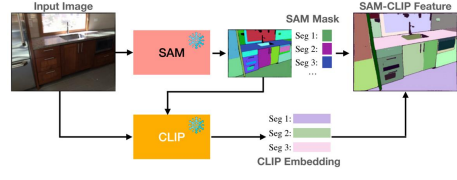
- 3D VLG faces significant data scarcity.
 - Only thousands of annotated scenes available.
 - High cost and time required for 3D annotations.
 - Limits scalability and performance of 3D VLG systems.

01 Bridging 2D and 3D: From Lifting to Learning



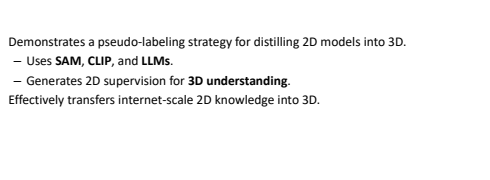
- Recent methods lift 2D models to 3D.
 - Suffer from slow optimization and accumulated errors.
 - Limited scalability.
 - Differentiable rendering offers a promising alternative.
 - Enables direct training of 3D models with 2D supervision.

02 Render-Supervised Training Pipeline



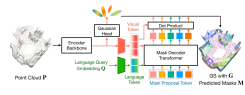
- LIFT-GS introduces a render-supervised training pipeline.
 - Requires only 2D supervision.
 - Eliminates need for scarce 3D annotations.
 - Uses differentiable rendering to train 3D models with 2D losses.

02 Pseudo-Labeling Strategy



- Demonstrates a pseudo-labeling strategy for distilling 2D models into 3D.
 - Uses SAM, CLIP, and LLMs.
 - Generates 2D supervision for 3D understanding.
 - Effectively transfers internet-scale 2D knowledge into 3D.

03 Task Formulation



- LIFT-GS predicts 3D Gaussian representations from point clouds.
 - Renders them into 2D views for supervision.
 - Allows training without 3D annotations.
 - Leverages 2D foundation models for pseudo-label generation.

03 Losses and Architecture

| Model | \mathcal{L}_{point} | \mathcal{L}_{clip} | \mathcal{L}_{cls} | Acc@0.5 | Acc@0.75 |
|---------|-----------------------|----------------------|---------------------|--------------|--------------|
| Scratch | ✓ | | | 42.19 | 23.96 |
| + | ✓ | ✓ | | 46.43 | 31.54 |
| + | ✓ | ✓ | ✓ | 46.67 | 31.81 |
| + | ✓ | ✓ | ✓ | 47.43 | 32.45 |
| + | ✓ | ✓ | ✓ | 47.53 | 31.36 |
| + | ✓ | ✓ | ✓ | 33.78 | 33.78 |

$$\mathcal{L}_{gross} = \frac{1}{K} \sum_i^K \lambda_1 \mathcal{L}_{mask}(\mathbf{M}_{gt}^i, \mathbf{M}_{pred}^i) + \lambda_2 \mathcal{L}_{cls}(\mathbf{C}_{gt(i)}, i) \quad (3)$$

$$\sigma(i) = \arg \min_j \mathbf{d}_{mask}(\mathbf{M}, \mathbf{M}_j, \mathbf{C}) \quad (4)$$

$$\mathcal{L}_{RGB} = \lambda_1 \mathcal{L}_1(I, \tilde{I}) + \lambda_2 \mathcal{L}_{SSIM}(I, \tilde{I}) \quad (6)$$

- Employs grounding losses and per-pixel losses.
 - Network-agnostic architecture.
 - Uses transformer-based grounding decoder.
 - Gaussian decoder head predicts 3D masks and features.

04 Training Details



- Trained on ScanNet and other datasets.
 - Uses 2D pseudo-labels and 3D annotations.
 - End-to-end optimization with differentiable rendering.
 - Various loss functions improve performance.

04 Evaluation on 3D Vision-Language Grounding

| Model | mAP \uparrow | mAP25 \uparrow | mAP50 \uparrow |
|----------------------------------|-----------------|------------------|------------------|
| OpenScene (Peng et al., 2023) | 11.7 | 17.8 | 15.2 |
| OpenMask3D (Takmaz et al., 2023) | 15.4 | 23.1 | 19.9 |
| PQ3D (Zhu et al., 2024) | 20.2 | 32.5 | 28.0 |
| LIFT-GS-Scratch | 22.5 | 35.1 | 30.7 |
| LIFT-GS | 25.7 | 40.2 | 35.0 |
| Δ | +3.2 \uparrow | +5.1 \uparrow | +4.3 \uparrow |

- Evaluated on 3D open-vocabulary instance segmentation.
- Shows significant improvements over state-of-the-art methods.
- Demonstrates effectiveness of pretraining approach.

Figure 15 Generated Sample 1, page 1 of 2.

Agent. We also include a biomedical-domain paper to demonstrate cross-domain generalization, with its generated slides shown in Figure 23. Additionally, Figure 14 shows a sample using the paper’s color palette as the theme color, including generated speaker notes.

11

05 / Grounding Simple Nouns in 3D

| Model | mAP↑ | mAP25↑ | mAP50↑ |
|----------------------------------|-------------|-------------|-------------|
| OpenScene (Peng et al., 2023) | 11.7 | 17.8 | 15.2 |
| OpenMask3D (Takmaz et al., 2023) | 15.4 | 23.1 | 19.9 |
| PQ3D (Zhu et al., 2024) | 20.2 | 32.5 | 28.0 |
| LIFT-GS-Scratch | 22.5 | 35.1 | 30.7 |
| LIFT-GS | 25.7 | 40.2 | 35.0 |
| Δ | +3.2 ↑ | +5.1 ↑ | +4.3 ↑ |

- LIFT-GS achieves substantial performance gains.
 - Outperforms state-of-the-art baselines.
 - Excels in open-vocabulary 3D instance segmentation tasks.

06 / Conclusion and Future Work

Conclusion

- LIFT-GS addresses data scarcity in 3D VLG.
 - Introduces **render-supervised distillation** from 2D VLM models.
- Achieves state-of-the-art performance.
 - Reveals substantial data limitations in 3D grounding.

Future Work

- Focus on improving **pseudo-labeling strategies**.
- Leverage advancements in 2D foundation models.
 - Enhance 3D model training and performance.

05 / Grounding Complex Phrases in 3D

| Method | SR3D | | NR3D | | ScanRefer | |
|---|-------------|-------------|-------------|-------------|-------------|-------------|
| | Acc@25 | Acc@50 | Acc@25 | Acc@50 | Acc@25 | Acc@50 |
| <i>Mesh PC</i> | | | | | | |
| 3D-VisRefer (Roh et al., 2021) | 59.5 | - | 28.6 | - | - | - |
| SAT-3D (Yang et al., 2023) | 35.4 | - | 31.7 | - | 44.5 | 30.1 |
| BUTD-DETR (Jain et al., 2021) | 52.1 | - | 43.3 | - | 52.2 | 39.8 |
| 3D-VisTA (Zhu et al., 2023c) | 56.5 | 51.5 | 47.7 | 42.2 | 51.0 | 46.2 |
| PQ3D (Zhu et al., 2024) | 62.0 | 55.9 | 52.2 | 45.0 | 56.7 | 51.8 |
| <i>Sensor PC + Bounding Box Proposals using Mesh PC</i> | | | | | | |
| 3D-VisTA (Zhu et al., 2023c) | 47.2 | 43.2 | 42.1 | 37.4 | 46.4 | 42.5 |
| <i>Sensor PC</i> | | | | | | |
| BUTD-DETR (Jain et al., 2021) | 43.3 | 28.9 | 32.2 | 19.4 | 42.2 | 27.9 |
| LIFT-GS-Scratch | 44.0 | 28.8 | 37.2 | 23.1 | 45.0 | 29.5 |
| LIFT-GS | 50.9 | 36.5 | 43.7 | 29.7 | 49.7 | 36.4 |
| Δ | +6.9(16%) | +7.7(27%) | +6.5(17%) | +6.6(29%) | +4.7(10%) | +6.9(23%) |

- Shows significant improvements in grounding complex phrases.
- Achieves state-of-the-art performance in 3D referential grounding.



Figure 16 Generated Sample 1, page 2 of 2.

E Samples Generated by baselines

Below are samples generated by baselines: Figure 24, 25, and 26.

F Template Library

The complete slide template library used by the Arranger can be seen in Figure 32. The selection rules are summarized in Table 9. These rules guide the Arranger module in choosing the most appropriate layout for each subsection based on the available images, tables, and formulas.

G Prompts

We provide the prompts used in our framework for reference, see Figures 34, 35, 36, 37, 38, 39, 40, 41, and 42.

H Example Output from Agents

Outliner Output

We provide example JSON outputs generated by Outliner, shown in Figures 43, 44, 45, 46, and 47.

Arranger Output

We provide example JSON outputs generated by Arranger, shown in Figures 48, 49, 50, 51, and 52.

Speaker Output

We provide example JSON outputs generated by Speaker, shown in Figure 53, 54, and 55.

Mapper Output

CLIP-DISSECT: Automatic Description of Neuron Representations in Deep Vision Networks

Tuomas Oikarinen, Tsui-Wei Weng

CONTENTS

01 Challenges in Understanding DNNs

- Deep neural networks excel in various domains.
- Understanding internal workings remains challenging.
 - Crucial for safety-critical tasks.
 - Helps identify potential biases.

02 Introduction to CLIP-Dissect

- CLIP-Dissect labels neurons with open-ended concepts.
- Uses multimodal models like CLIP.
- Does not require labeled data.
- Model-agnostic and computationally efficient.

02 Advantages Over Existing Methods

| Metric | Similarity function | D_{probe} | | | | |
|----------------|---------------------|----------------|---------------|---------------|-----------------------|---------------|
| | | CIFAR100 train | Broden | ImageNet val | ImageNet val + Broden | Average |
| mpnet | cos | 0.2761 | 0.215 | 0.2823 | 0.2584 | 0.2580 |
| cos similarity | Rank reorder | 0.3250 | 0.3857 | 0.4901 | 0.5040 | 0.4262 |
| WPMI | WPMI | 0.3460 | 0.3878 | 0.5302 | 0.5267 | 0.4477 |
| SoftWPMI | SoftWPMI | 0.3664 | 0.3945 | 0.5257 | 0.5233 | 0.4525 |
| Top1 accuracy | cos | 8.50% | 5.70% | 15.90% | 11.40% | 10.38% |
| | Rank reorder | 36.30% | 57.50% | 89.80% | 89.90% | 68.38% |
| | WPMI | 23.80% | 47.10% | 87.00% | 86.90% | 61.20% |
| | SoftWPMI | 46.20% | 70.50% | 95.00% | 95.40% | 76.78% |

- CLIP-Dissect provides accurate neuron descriptions.
- Significantly faster than existing methods.
- Handles new concepts flexibly.

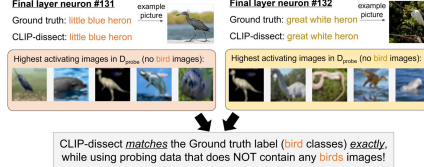
03 Similarity Function Choices

- Various similarity functions explored.
- SoftWPMI performs best.
 - Considers probability of images belonging to a concept.

| Metric | Similarity function | D_{probe} | | | | |
|----------------|---------------------|---------------|---------------|---------------|---------------|---------------|
| | | CIFAR100 | Broden | ImageNet | ImageNet val | Average |
| impact | cos | 0.3490 | 0.3113 | 0.2523 | 0.2584 | 0.3201 |
| cos similarity | Rank reorder | 0.3795 | 0.3893 | 0.4823 | 0.4829 | 0.4282 |
| WPMI | WPMI | 0.3460 | 0.3878 | 0.5302 | 0.5267 | 0.4477 |
| SoftWPMI | SoftWPMI | 0.3664 | 0.3945 | 0.5257 | 0.5233 | 0.4525 |
| Top1 accuracy | cos | 8.50% | 5.70% | 15.90% | 11.40% | 10.38% |
| | Rank reorder | 36.30% | 57.50% | 89.80% | 89.90% | 68.38% |
| | WPMI | 23.80% | 47.10% | 87.00% | 86.90% | 61.20% |
| | SoftWPMI | 46.20% | 70.50% | 95.00% | 95.40% | 76.78% |

$$\text{sim}(t_m, q_k; P) \triangleq \frac{P_m^T q_k}{\|P_m\| \cdot \|q_k\|} \quad (1)$$

04 Detecting Concepts Beyond Probing Images



- Correctly labels neurons without direct image probes.
- Showcases robustness of CLIP-Dissect.

Figure 17 Generated Sample 2.

We provide example JSON outputs generated by Mapper, shown in Figure 56 and 57.

Formulizer Output We provide example JSON outputs generated by Formulizer, shown in Figure 58.

Denoising MCMC for Accelerating Diffusion-Based Generative Models

Beomsu Kim; Jong Chul Ye

CONTENTS

- 1. Motivation And Problem Formulation
- 2. Background On Scores, MCMC, And Diffusion
- 3. Key Contributions And High-Level Idea
- 4. Method Overview And Algorithmic Steps
- 5. Technical Details And Practical Choices
- 6. Experiments, Datasets, And Integrators

01 Why Accelerate Diffusion Sampling?

- Reverse S/ODE sampling needs hundreds-thousands of score evaluations.
- High compute hinders high-resolution, diverse generation.
- Traditional MCMC mixes poorly in high-dimensional, multimodal manifolds.
- Goal: faster sampling without sacrificing fidelity or diversity.

02 Diffusion Models, Reverse SDEs And ODEs

$$dx = f(x, t) dt + g(t) dw \quad (2)$$

$$dx = [f(x, t) - g(t)^2 \nabla_x \log p_t(x)] dt + g(t) dw \quad (3)$$

- Forward diffusion admits reverse SDE and probability-flow ODE.
- Integrating reverse dynamics with scores yields samples.
- VE and VP are equivalent via change-of-variables; solver choice matters.

03 Denoising MCMC: Product-Space Initialization

- Propose DMCYC: MCMC over (data, noise) then short reverse integration.
- Chains dwell near manifold at low noise, shortening integration interval.
- Enables faster, high-fidelity sampling under tight NFE budgets.

03 Key Contributions And High-Level Idea

Denoising Langevin Gibbs (DLG) Instance

DLG alternates Langevin x-updates and σ -updates via classifier. Requires pretrained score and lightweight noise-level classifier. Compatible with any reverse S/ODE; works for VE or VP scores.

Orthogonality To Solver Improvements

DMCYC provides better initialization, complementing solver advances. Combining DMCYC with improved integrators further boosts performance. Enhances predictor-corrector by strengthening initialization quality.

04 Step 1: MCMC On Data–Noise Product Space

$$dx = [f(x, t) - (1/2) \cdot g(t)^2 \nabla_x \log p_t(x)] dt \quad (4)$$

$$d\sigma = \sqrt{\frac{|d\sigma^2(t)|}{dt}} dw \quad (5)$$

- Define joint target over data and noise with smoothing and prior.
- MCMC samples (x, σ) , moving up for mixing and down near manifold.
- Prior can bias toward small σ while preserving mixing.

04 DLG: Alternating Langevin And Noise Prediction

- Langevin step uses conditional score at current σ .
- Predict next σ via classifier approximating $p(\sigma|x)$.
- Select lowest- σ state per block for denoising.

05 Technical Details And Practical Choices

Warm Starts, Skipping, And Selection

Warm start: generate clean, add noise, run few Gibbs updates. Reduce autocorrelation by processing every $n_{\text{skip-th}}$ block. Within blocks, pick minimum- σ state for denoising. Allocate NFEs between chain and denoising for balance.

Choice Of Prior And Hyperparameters

Use 1/o prior to nudge toward low noise while mixing. Overly sharp priors slow convergence; trade-offs exist. Tune step size η and denoising NFE ratio jointly.

06 Mixing And Mode Coverage

Figure 18 Generated Sample 3, page 1 of 2.

I Color Setting

We control the theme color choices with a three-step procedure that combines fixed safety constraints with light refinement by Refiner.

Step 1: Human-defined baseline. We start with a set of baseline parameters that guide color adjustments in HSV space. These include the target saturation level, minimum and maximum saturation values, desired brightness for dark themes, and a fallback hue for colors that are nearly gray. We set this baseline once to ensure stable results: colors avoid becoming too bright, dull, or extreme. This baseline also sets "safe ranges" to prevent later changes from creating unusable colors.

Step 2: LLM-based refinement. Next, we feed these baseline parameters-along with a brief style description string, such as "dark academic, calm, professional", into Refiner. The agent does not create final colors itself. Instead, it suggests small, style-focused tweaks to the parameters (for example, slightly reducing the brightness target or increasing the minimum saturation). These tweaks stay within the safe ranges and are applied only once at the start. This step brings in the language model's sense of style while keeping colors controlled.

Step 3: Deterministic color generation. With the refined parameters in place, all final slide colors are generated deterministically by our HSV Adjustment Algorithm 3.

In summary, this combined method uses the strengths of language models for interpreting style descriptions, while making the overall slide generation reliable, consistent, and easy to repeat.

Algorithm 3: Detailed Color Movement Rules on the HSV Plane

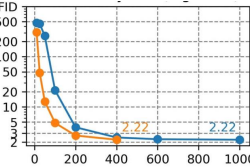
Input : HSV (H, S, V) with $S, V \in [0, 1]$; parameters: **satTarget**, **satFloor**, **satCap**, **satBlend**, **targetV**, **vCap** (optional), **gamma**, **fallbackHue**

Output : Updated (H, S, V)

```
/* Parameters: */  
/* satTarget (0..1): target saturation you want to push toward. */  
/* satFloor (0..1): minimum allowed saturation to avoid muddy gray. */  
/* satCap (0..1): maximum allowed saturation to prevent neon look. */  
/* satBlend (0..1): how strongly  $S$  moves toward satTarget each step. */  
/* targetV (0..1): desired brightness “baseline” for a dark theme. */  
/* vCap (0..): brightness ceiling after darkening. */  
/* gamma (> 0): adaptive strength; the brighter above targetV, the more  $V$  moves down. */  
/*  
If the color is nearly gray ( $S \approx 0$ ): set  $H$  to the hue of fallbackHue (#2B5FA6) and raise  $S$  to at least satFloor ;  
Move right (make it more vivid, but not too much):  
  if  $S < \text{satTarget}$  or  $S < \text{satFloor}$  then  
     $S \leftarrow (1 - \text{satBlend}) \cdot S + \text{satBlend} \cdot \text{satTarget}$ ;  
     $S \leftarrow \text{clamp}(S, \text{satFloor}, \text{satCap})$ ;  
Move down (darker adaptively: the brighter it is, the more it moves):  
  if  $V > \text{targetV}$  then  
     $d \leftarrow V - \text{targetV}$ ;  
     $a \leftarrow 1 - e^{-\text{gamma} \cdot d}$  ;  
     $V \leftarrow V - a \cdot d$  ;  
    // bigger gap  $\Rightarrow$  stronger pull  
    // pull  $V$  toward targetV  
    if vCap is set then  
       $V \leftarrow \min(V, \text{vCap})$   
Optional gentle lift (avoid being too dark):  
  Let vFloor = targetV - 0.02.  
  if  $V < \text{vFloor}$  then  
     $V \leftarrow 0.7 \cdot V + 0.3 \cdot \text{vFloor}$   
return  $(H, S, V)$ ;
```

06 / Image Generation Benchmarks

- DLG accelerates multiple samplers across CIFAR-10, CelebA-HQ, FFHQ.
- Reduces NFEs needed for competitive or better FID.
- Works for deterministic and stochastic integrators.



06 / Conditional Generation And Scores

| Class | 0 | 1 | 2 | 3 | 4 | 5 | 6 | 7 | 8 | 9 |
|----------|------|------|------|------|------|------|------|------|------|------|
| No DLG | 14.3 | 11.6 | 15.8 | 17.7 | 14.7 | 16.9 | 16.0 | 13.4 | 11.1 | 11.3 |
| With DLG | 12.2 | 9.3 | 13.5 | 14.8 | 11.6 | 13.6 | 12.7 | 10.6 | 9.3 | 8.5 |

- DLG improves class-conditional generation with VE and VP scores.
- Per-class FID improves when adding DLG to same integrator.

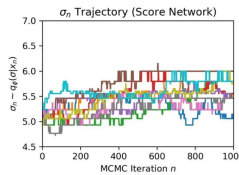
07 / State-Of-The-Art In Low-NFE Regime

| Method | NFE 10 | NFE 20 | NFE 50 |
|-------------------|------------------------|------------------------|-------------------------|
| DPM-Solver-2 (VP) | 5.28 (+2 NFE) | 3.02 (+4 NFE) | 2.69 (~2 NFE) |
| DPM-Solver-3 (VP) | 6.03 (+2 NFE) | 2.75 (+4 NFE) | 2.65 (~2 NFE) |
| DEIS (VP) | 4.17 (+0 NFE) | 2.86 (+0 NFE) | 2.57 (+0 NFE) |
| DEIS (VE) | 20.89 (+0 NFE) | 16.59 (+0 NFE) | 16.31 (+0 NFE) |
| KARI (VP) | 9.70 (+1 NFE) | 3.23 (+5 NFE) | 2.97 (+1 NFE) |
| KARI (VE) | 14.12 (+1 NFE) | 4.46 (+5 NFE) | 4.1 (+1 NFE) |
| DLG+KARI (VP) | 3.25 (+0.1 NFE) | 2.49 (~3.9 NFE) | 2.49 (~33.9 NFE) |
| DLG+KARI (VE) | 3.86 (+0.1 NFE) | 2.63 (+0.1 NFE) | 2.45 (~0.9 NFE) |

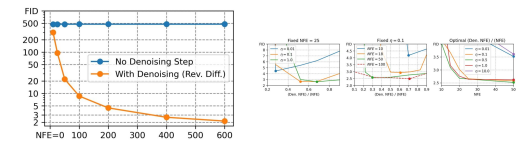
- DLG+KARI achieves SOTA FID at ~10-16 NFE on CIFAR-10.
- CelebA-HQ: 256: DLG+KARI2 outperforms prior 4000+ NFE results.
- FFHQ: 1024 shows large low- NFE FID gains.

07 / σ -Trajectory And Manifold Proximity

- σ trajectories move up/down, enabling mode transitions.
- Predicted σ correlates with distance to manifold scaling.
- Classifier keeps chains where score gradients are informative.



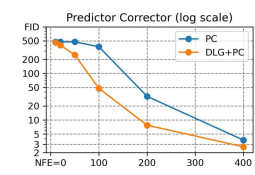
07 / Ablations: η , NFE Split, And Necessity Of Denoising



- Optimal η and denoising- to- total NFE ratio balance diversity and quality.
- As NFE grows, near-optimal ratios widen.
- Removing denoising collapses quality—denoising is essential.

08 / Relation To Predictor-Corrector And Distillation

- DMCMC complements PC by improving initialization; accelerates PC pipelines.
- Compared to distillation, requires far less extra training compute.
- Achieves competitive FID at similar NFE with minimal overhead.



08 / Related Work, Limitations, And Impact

Limitations And Future Extensions

Extensions to guided diffusion (classifier/CLIP) Acceleration reduces compute and energy for generative models.

Further theory on Langevin Gibbs convergence and adaptive priors needed.

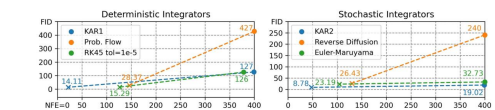
Trade-offs between stability and speed warrant deeper analysis.

Societal Impacts And Reproducibility

Faster sampling can amplify misuse risks; responsible deployment is needed.

Code and checkpoints provided with clear hyperparameters and pseudocode.

09 / Main Takeaways



- DMCMC samples in data-time space first, then denoises, shortening integration.
- DLG is simple, plug-and-play, and scales to high resolution.
- Delivers state-of-the-art results in low-NFE regimes.

Figure 19 Generated Sample 3, page 2 of 2.

Simplex Random Features

Isaac Reid; Krzysztof Choromanski; Valerii Likhoshesterov; Adrian Weller

CONTENTS

1. Motivation And Background
2. Related Work And Orthogonality Gap
3. Key Contributions
4. Method Overview
5. Technical Details And Optimality
6. Experiments And Datasets

01 Why Random Features For Kernels?

- Random features approximate nonlinear kernels with scalable linear operations.
- IID sampling yields high-variance estimator coupling directions reduces MSE.
- ORFs correlate directions via orthogonality; used for linear-time attention.
- PRFs and softmax/Gaussian kernels are primary targets.

$K(x, y) = \mathbb{E}[\tilde{K}(x, y)]$, where $\tilde{K}(x, y) \stackrel{\text{def}}{=} \phi(x)^\top \phi(y)$.

02 Structured Random Features Landscape

| | Time-complexity | SimRFs | SimRFs+ |
|---------|-------------------------|-------------------------|--------------------|
| Regular | $\mathcal{O}(d^3)$ | $\mathcal{O}(d^3)$ | $\mathcal{O}(d^3)$ |
| Fast | $\mathcal{O}(d \log d)$ | $\mathcal{O}(d \log d)$ | $\mathcal{O}(d^3)$ |

- Structured transforms (JLT, Fastfood, HDI) enable fast RFs.
- ORFs show benefits of orthogonal correlation.
- Non-asymptotic PRF forms were lacking; Performers inherit ORF suboptimality.

03 Simple Random Features (SimRFs)

- SimRFs align directions with a regular simplex, randomized by Haar rotations.
- Independent χ -distributed norms preserve Gaussian marginals.
- Provably minimize PRF MSE among weight-independent couplings; beat ORFs.

$d = 2$

$d = 3$

IIDRFs ORFs SimRFs

$K_{\max}(x, y) \stackrel{\text{def}}{=} \exp(x^\top y)$. (5)

04 Geometrical Coupling And RF-Conformity

- Define RF-conformity $p(x, y)$; estimator MSE increases with p .
- Geometrical coupling correlates directions with independent or dependent norms.

$\text{Probability distributions over } w_{ki}, d=6$

$\text{MSE}(\tilde{K}) = \frac{e^{-2\pi^2 \sigma^2}}{m} \left((e^{2\pi^2 \sigma^2} - e^{\sigma^2}) + (m-1)(p(x, y) - e^{\sigma^2}) \right)$. (11)

05 SimRFs+ And Theoretical Advances

- Orthogonality shrinks heavy tails of resultant sums, lowering MSE versus IID.
- A positive orthogonality gap remains; better couplings can further reduce MSE.

MSE ratio between RF mechanisms

06 SimRFs+ And Theoretical Advances

- SimRFs+ adapts angles to sampled norms; slight gains, small- v optimality.
- First non-asymptotic PRF MSE closed forms for IID, ORF, SimRF.
- Extensions to RFFs and discussion of fast implementations.

07 Geometrical Coupling And RF-Conformity

- Define RF-conformity $p(x, y)$; estimator MSE increases with p .
- Geometrical coupling correlates directions with independent or dependent norms.

$\text{Probability distributions over } w_{ki}, d=6$

$\rho(x, y) = \frac{\Gamma(\frac{d}{2})}{m(m-1)} \sum_{i,j \in S} \left(\sum_{k=0}^m \frac{e^{2\pi^2 \sigma^2}}{2^{2k} k! \Gamma(k+\frac{d}{2})} \right)$. (12)

08 Simplex Block Construction

- Construct $W = D S R$ with x norms D , Haar orthogonal R , simplex directions S .
- Fixed obtuse angles $\cos \theta = -1/(d-1)$ reduce pairwise resultants and conformity.

$d = 2$

$d = 3$

IIDRFs ORFs SimRFs

PART 01

Motivation And Background

PART 02

Related Work And Orthogonality Gap

PART 03

Key Contributions

PART 04

Method Overview

PART 05

Technical Details And Optimality

Figure 20 Generated Sample 4, page 1 of 2.

18

05 / Theorem: MSE Increases With RF-Conformity

- PRF estimator MSE = base term + conformity-dependent term.
- Reducing $\|w_i \mathbf{1} + w_i\mathbf{1}\|$ lowers p and strictly reduces MSE.

05 / SimRFs Versus ORFs

- SimRFs enforce $\cos\theta = -1/(d-1)$ vs ORF orthogonality ($\cos\theta=0$).
- Closed-form p enable precise non-asymptotic MSE comparisons.

05 / SimRFs+: Weight-Dependent Coupling

$$\mathbf{w}_i \leftarrow -\frac{\sum_{j \neq i} \mathbf{w}_j}{\left(\sum_{j \neq i} \mathbf{w}_j\mathbf{1}\right)^\top \mathbf{w}_i} \quad (17)$$

$$p_{i,i}(\mathbf{w}_i) = \frac{\mathbf{w}_i^\top \mathbf{w}_i}{2^{d-1} \Gamma(d)} \quad (18)$$

- Minimize truncated conformity; larger-norm vectors get larger angles.
- Iterative updates converge quickly from simplex initialization; gains are marginal.

05 / Extension To RFFs And Complexity

where $\mathbf{x}, \mathbf{y} \in \mathbb{R}^d$ and $v = \|\mathbf{x} + \mathbf{y}\|_2$.

PART 06

Experiments And Datasets

06 / Nonparametric Classification

- Kernel regression: SimRFs achieve higher accuracy, converging to exact kernel.
- SimRFs+ gives minor gains in small-v regimes; σ tuned via validation.

06 / Pointwise MSE And Gram Matrix Approximation

- Analytic MSE curves: SimRFs beat ORFs and IID, especially at small v.
- Gram approximation shows lower Frobenius error across feature counts.

PART 07

Results And Analysis

06 / Transformers: SimRFs-Performer

- Replacing ORFs with SimRFs in Performer improves or matches accuracy.
- Gains observed on ImageNet2012, Fashion-MNIST, iNaturalist2021, Places365.

07 / Closed-Form MSE Comparisons

- Non-asymptotic closed forms quantify conformity and MSE gaps.
- Tall suppression hierarchy: SimRFs < ORFs < IIDRFs.

PART 08

Conclusion And Future Work

07 / Cost And Practicality

| | Time-complexity |
|---------|-------------------------|
| ORFs | $\mathcal{O}(d^3)$ |
| SimRFs | $\mathcal{O}(d^3)$ |
| SimRFs+ | $\mathcal{O}(d^3)$ |
| Regular | $\mathcal{O}(d^3)$ |
| Fast | $\mathcal{O}(d \log d)$ |

- SimRFs are near drop-in replacements for ORFs with similar cost.
- Structured orthogonal proxies keep accuracy while reducing matvec cost.
- SimRFs+ adds overhead with marginal returns.

08 / Main Takeaways

- SimRFs optimally minimize PRF MSE among weight-independent couplings.
- They strictly outperform ORFs without added cost; SimRFs+ offers slight gains.
- Empirical results corroborate theory across tasks.

Geometrically-coupled

$\text{IIDRFs} < \text{ORFs} < \text{SimRFs} < \text{SimRFs+}$

Weight-independent Weight-dependent

THANKS!

19

Figure 21 Generated Sample 4, page 2 of 2.

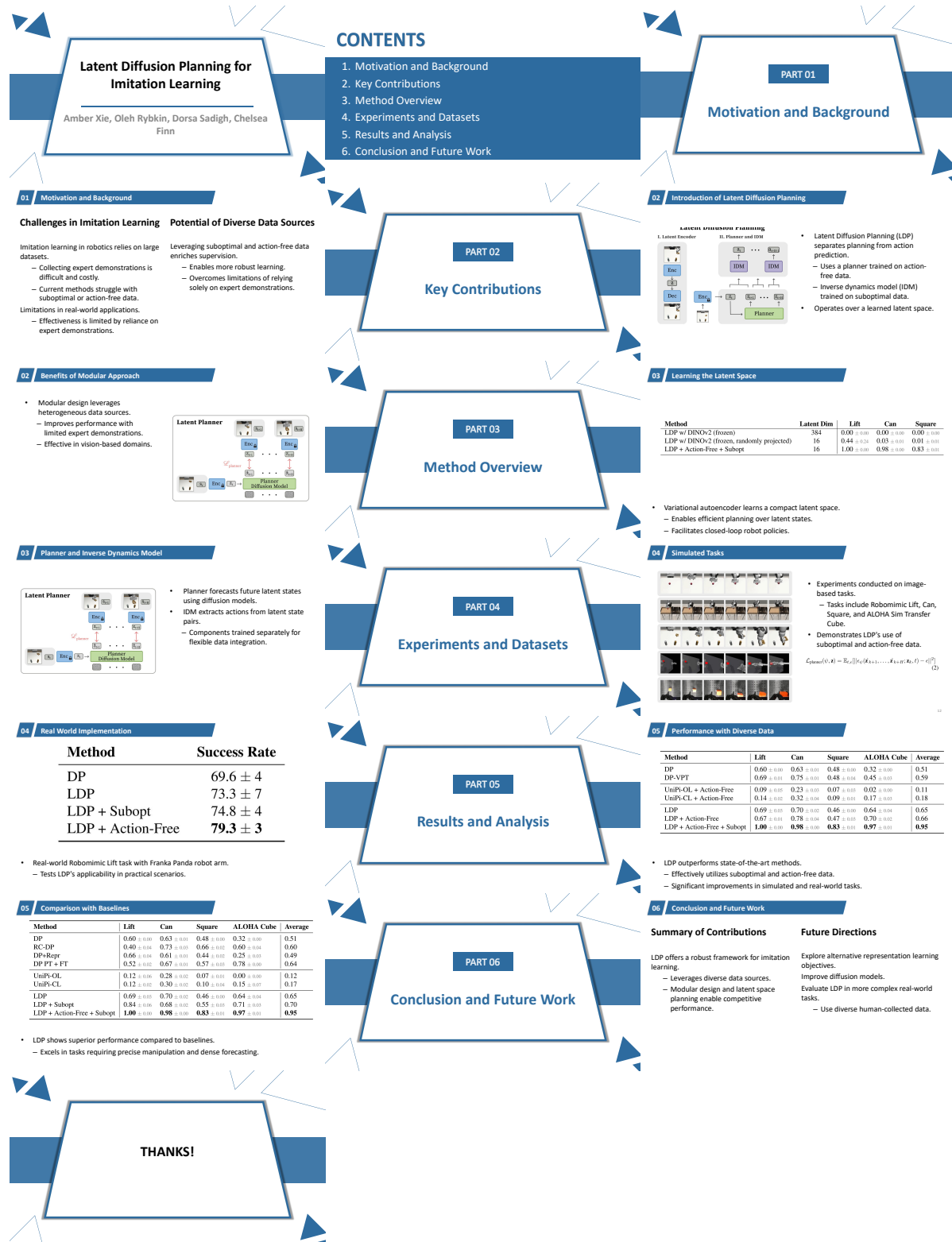


Figure 22 Generated Sample 5.

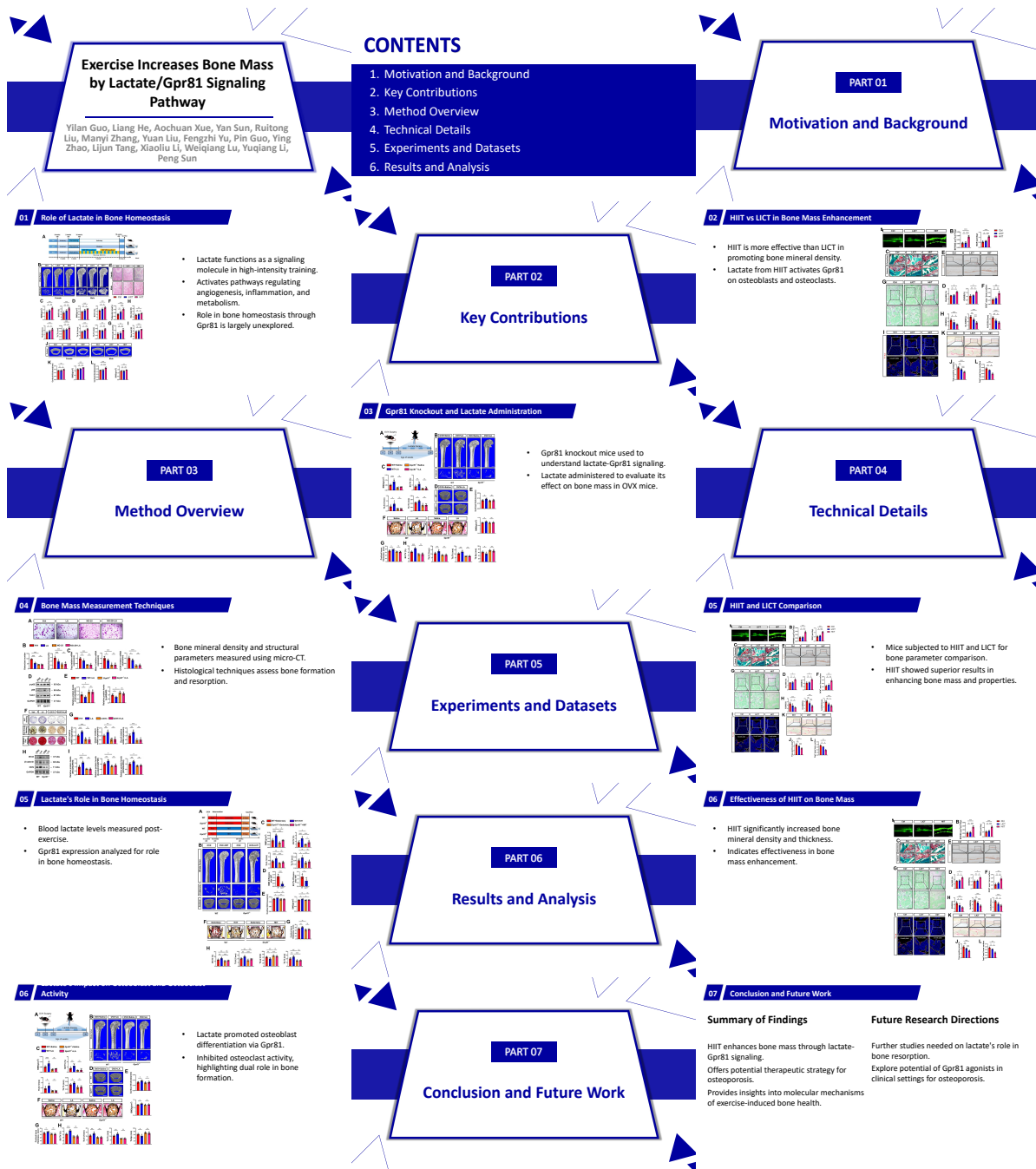


Figure 23 Generated Sample 6 in biomedical domain.

The In-Sample Softmax for Offline Reinforcement Learning

Chenjun Xiao,¹ Hani Wang¹, Yangchen Pan, Adam White²

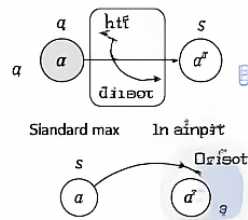
¹ Hapti² Kort E Ar³ Lo⁴

² University of Alberta, Alberta Machine Intelligence Institute (Amii)

³ University of Oxford

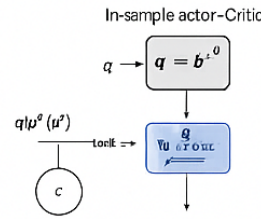
Motivation

- Introduced in-sample softmax in actions
- Constraint on-set actions
- Proposal on better performance



In-Sample Actor-Critic

- Method In-Sample
- Update Method
- Entropy optimization
- Using entropy
- Full offline training with Online fine-tuning



Training Results

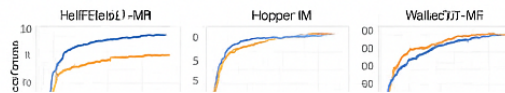


Figure 24 A generated Sample by ChatGPT-4o.

Introduction

- Use of batches of previous the dataset
- Proposal on in-sample softmax action considered and before the first
- Proposal of comparable or better

In-Sample Softmax

- Q₁ in-sample max
- Policy Iteration
- Action-values
- Convergence to in-sample max

$$q_{IS}(i) = \rho_{1i} \frac{\pi^*(i)}{\pi^*}$$

$$\pi^*(i) = \sum_{j \in A} \pi^*(i, j)$$

$$\pi^*(i) = \sum_{j \in A} \frac{1}{\pi^*(i, j)}$$

Experimental Setup

| | MuleCo | Baselines |
|---------------|--------|-----------|
| BC | 6.6 | 16.1 |
| COL | 3.0 | 12.2 |
| IOL | 10.1 | 17.1 |
| IO2 + F | 6.3 | 10.0 |
| (Pofalk) | 4.6.2 | 3.8.9 |
| medium-replay | 8.6.3 | 8.6.5 |
| medium-replay | 9.6.2 | 8.5.5 |
| medium-replay | 6.6.2 | 9.9.4 |

Fine-Tuning Results

- Introduced in-sample softmax actions in dataset
- In-sample actor critic provided convergent

DocPrompting

Generating Code by Retrieving the Docs

Jin Zou, Uri Alon, Frank F Xu, Zhiruo Wang
Zhengbao Liang, Graham Keubig
Language Technologies Institute, Carnegie Mellon University
@loup, alihoubig@cs.cmu.edu

Introduction

Existing NL-to-code models require a large amount of pre-existing code repositories. Human programmers frequently refer to documentation to find informed data.

Method

Flowchart illustrating the DocPrompting process:

```

graph LR
    A[Input Intent] --> B[Retriever]
    B --> C[Generator]
    C --> D[Generated]
    B --> D1[d7]
    C --> D2[d1-d3]
  
```

• 2-step process: retrieve documentation and generate code.

Conclusion

• Discussed: code deletion/recursion issues.

• Introduced DocPrompting as retrieving documentation and leveraging documentation in NL-to-code models.

Related Work

Existing NL-to-code models focus on pairs specific to certain code.

Models that reuse existing libraries or function calls are less effective.

Results: Python CoNaLa

| | DocPrompt | DP_Promp |
|---------------|-----------|----------|
| Code15 | 5.4% | 3.63% |
| GPT-Neo-1.3 B | 3.3% | 5.48% |

Results: Bash TLDR

| | DocPrompt | DP_Promp |
|---------------|-----------|----------|
| Code15 | 4.2% | 5.68% |
| GPT-Neo-1.3 B | 4.9% | 5.37% |

Figure 25 A generated Sample by ChatGPT-5.



Figure 26 A generated Sample by ChatGPT-4o-HTML.

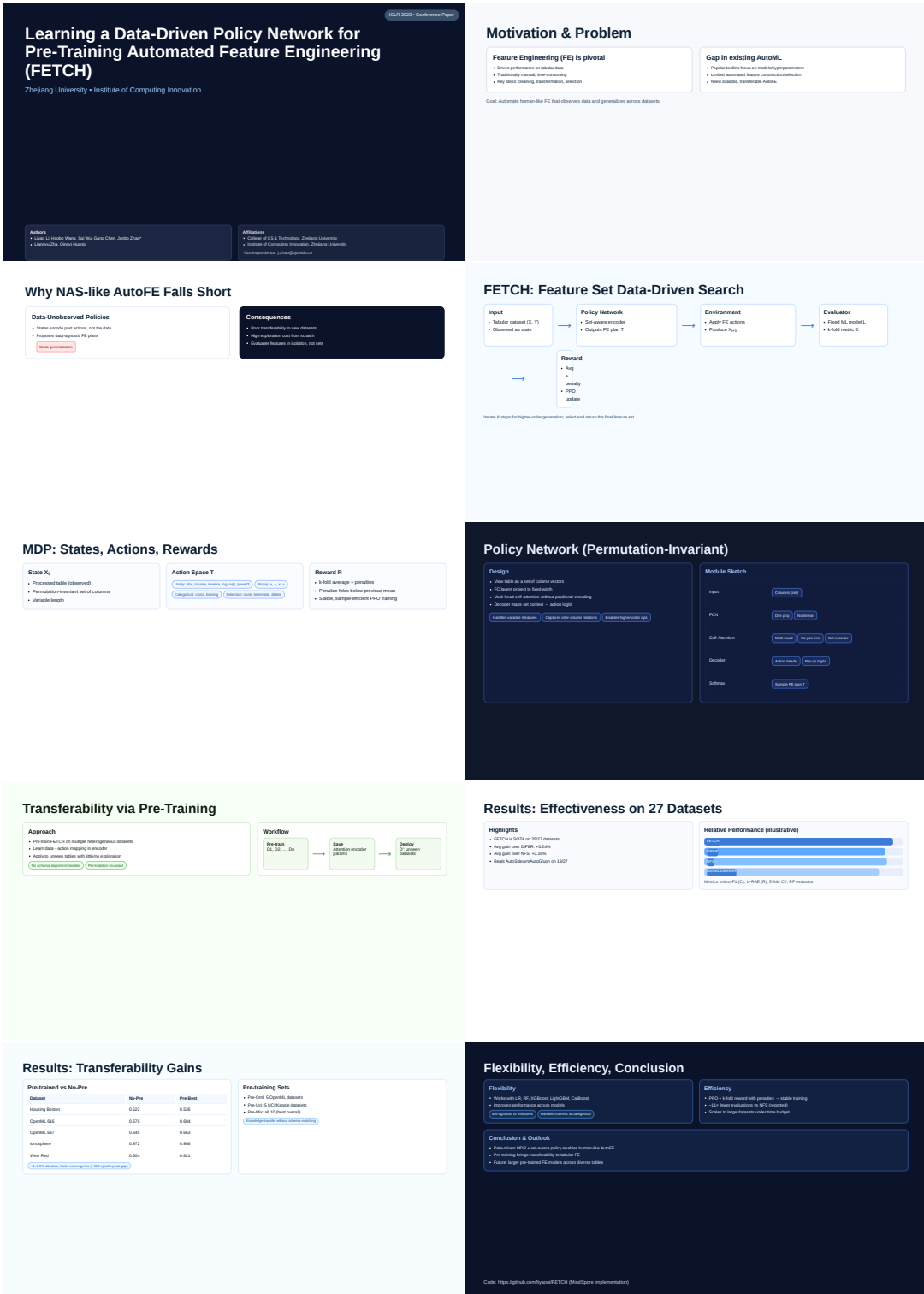


Figure 27 A generated Sample by ChatGPT-5-HTML.

```

generate_question_detail

system_prompt: |
You are a Question-Generation agent for academic slides.
Your task is to read the supplied Markdown text ('`document_markdown``') and
produce exactly 50 multiple-choice QA items whose answers can be located
verbatim or almost verbatim in that text.
The questions must be suitable for conference-slide-deck readers: avoid deep
theoretical proofs, reference lists, or citation minutiae.
Follow all guidelines below precisely.

template: |
=====
INSTRUCTIONS
=====
1. Carefully read the Markdown in ``document_markdown``.
2. Write 50 factual, answerable-from-text questions.


- Each question must map to one clear sentence/phrase in the slide-deck text.
- No duplicate or near-duplicate wording.
- Vary difficulty from easy “headline” facts to specific numeric or
procedural details.


3. Distribute the 50 questions across the following slide-deck-friendly aspects.
Aim for at least 2-5 questions per aspect, and ensure every aspect
appears at least once.


- A. Title & authorship (title, author names, affiliations, keywords)
- B. Motivation / problem statement / research gap
- C. Objectives or hypotheses
- D. Dataset(s) or experimental materials
- E. Methodology (algorithms, model architecture, workflow steps)
- F. Key parameters or hyper-parameters (values, settings)
- G. Evaluation metrics or criteria
- H. Quantitative results (numbers in tables, charts)
- I. Qualitative findings, figures, or illustrative examples
- J. Comparative or ablation study results
- K. Conclusions, implications, or contributions
- L. Limitations or future work
- M. Definitions of domain-specific terms or abbreviations


4. EXCLUDE references, citations, author acknowledgements, and any text
that would not appear on a standard slide-deck.
5. Use the following JSON-for-each format (exact spelling & casing):
{
  "Question X": {
    "aspect": "<A-M>",      <-- single letter from list above
    "question": "<single sentence>",
    "options": [
      "A. <choice 1>",
      "B. <choice 2>",
      "C. <choice 3>",
      "D. <choice 4>"
    ],
    "answer": "<Letter>. <exact correct option text>"
  }
}

```

Figure 28 The complete prompt used to construct both verbatim and interpretive questions, page 1 of 4.

```
},
...
}
Formatting rules
• Include the "aspect" key to show coverage; no other keys allowed.
• Exactly four options labelled A-D.
• Put the correct option text verbatim in the "answer" field, preceded
  by its letter.
• Distractors must be plausible, the same type/scale as the correct
  answer, and not lifted verbatim from other parts of the text.
6. Output only the final JSON object containing 50 items—nothing else.
7. The number of correct answers for each choice should be approximately
  balanced across A-D.
```

```
document_markdown:
{{ document_markdown }}
```

Return ONLY the JSON with 50 questions below

```
jinja_args:
- document_markdown
```

Figure 29 The complete prompt used to construct both verbatim and interpretive questions, page 2 of 4.

```

generate_question_understanding

system_prompt: |
You are a Question-Generation agent.
Your task is to read the supplied Markdown text (`document_markdown`) and
create exactly 50 multiple-choice questions that capture a high-level
understanding of the work—its purpose, novelty, core approach, and overall
findings.
Every question must still be answerable by locating explicit sentences or
phrases in the text; do not require inference that is absent from the slide-
style content.

template: |
=====

INSTRUCTIONS
=====

1. Read the Markdown in ``document_markdown`` closely.
2. Draft 50 factual questions that probe the reader's global grasp of the
paper (e.g., "What problem does the study address?").


- Avoid low-level numeric settings, code snippets, or reference lists.
- Vary wording and avoid duplicates.


3. Cover all of the following high-level aspects—each must appear at least
twice to guarantee breadth:


- Research domain & background context
- Central problem / motivation / research gap
- Primary goal, hypothesis, or research question
- Key contributions or novelty statements
- Overall methodology or workflow (summarized)
- Principal findings or headline quantitative results
- Qualitative insights or illustrative examples
- Implications, applications, or significance
- Limitations or future-work directions
- Main conclusions or take-home messages


4. EXCLUDE citations, granular hyper-parameters, precise numeric tables, and
acknowledgements—stick to slide-level overview content.
5. Return the questions in the following strict JSON schema:
{
  "Question X": {
    "aspect": "<A-J>",           <-- single capital letter above
    "question": "<one concise sentence>",
    "options": [
      "A. <choice 1>",
      "B. <choice 2>",
      "C. <choice 3>",
      "D. <choice 4>"
    ],
    "answer": "<Letter>. <exact correct option text>"
  },
  ...
}
Formatting rules

```

Figure 30 The complete prompt used to construct both verbatim and interpretive questions, page 3 of 4.

- Exactly four labelled options (A-D); one is correct.
- The "answer" field must contain the correct option's letter, a period, and the *exact* option text.
- Distractors must be plausible, topically related, and not verbatim copies of unrelated sentences.

6. Produce **only** the final JSON object with 50 entries—no commentary, headers, or extra lines.

7. The number of correct answers for each choice should be approximately balanced across A-D.

```
document_markdown:
{{ document_markdown }}
```

Output ONLY the JSON with 50 questions below

```
jinja_args:
- document_markdown
```

Figure 31 The complete prompt used to construct both verbatim and interpretive questions, page 4 of 4.

Table 9 Summary of slide templates and their selection rules used by the Arranger.

| Template | Selection Rule |
|---|--|
| T1_TextOnly | Use when the subsection contains no images or tables; suitable for pure-text slides or conceptual summaries. |
| T2_ImageRight | One tall/square image (aspect ≤ 1.0) + up to four bullets. Image placed on the right, text on the left. |
| T3_ImageLeft | Mirror of T2. One tall/square image placed on the left, text on the right. |
| T4_ImageTop | One wide image/table (aspect ≥ 1.6) or any visual that spans nearly the slide width; image on top, text below. |
| T5_TwoImages | Exactly two images side-by-side, with no text. Suitable for visual comparison. |
| T5_TwoImages2 | Two side-by-side images on top, with a text block underneath. |
| T7_2x2_TopImage | 2x2 layout: top two blocks are images, bottom two are text. For two visuals + explanatory bullets. |
| T8_2x2_BottomImage | 2x2 layout: top two blocks are text, bottom two are images. Use when the narrative is text-heavy. |
| T9_2x2_AltTextImg | Alternating 2x2 layout (top-left & bottom-right = images; top-right & bottom-left = text). |
| T10_4Img_2x2Grid | Exactly four images in a 2×2 grid, with no text. Best for dataset galleries or qualitative comparisons. |
| T11_3Img_TopTextBottom | Three images in one row across the top with a text block below. |
| T12_3Img_BottomTextTop | Text block on top followed by three images in a row. |
| T13_3Img | Title on top with three evenly spaced images below. |
| T14_ImageRight_1Formula | Right column contains one image/table (top) + one formula (bottom); text on the left. For paired visual + equation slides. |
| T15_ImageLeft_1Formula | Mirror of T14: image/table + formula on the left column; text on the right. |
| T16_1Img_2formula_-TopTextBottom | Top rows contain one image/table + two formulas; text block at the bottom. |
| T17_2Img_1formula_-TopTextBottom | Two images on the top row, one formula in the middle, text at the bottom. |
| T18_2formula_-TopTextBottom | Two formulas stacked at the top with a text block below. Use when both formulas belong on the same slide. |

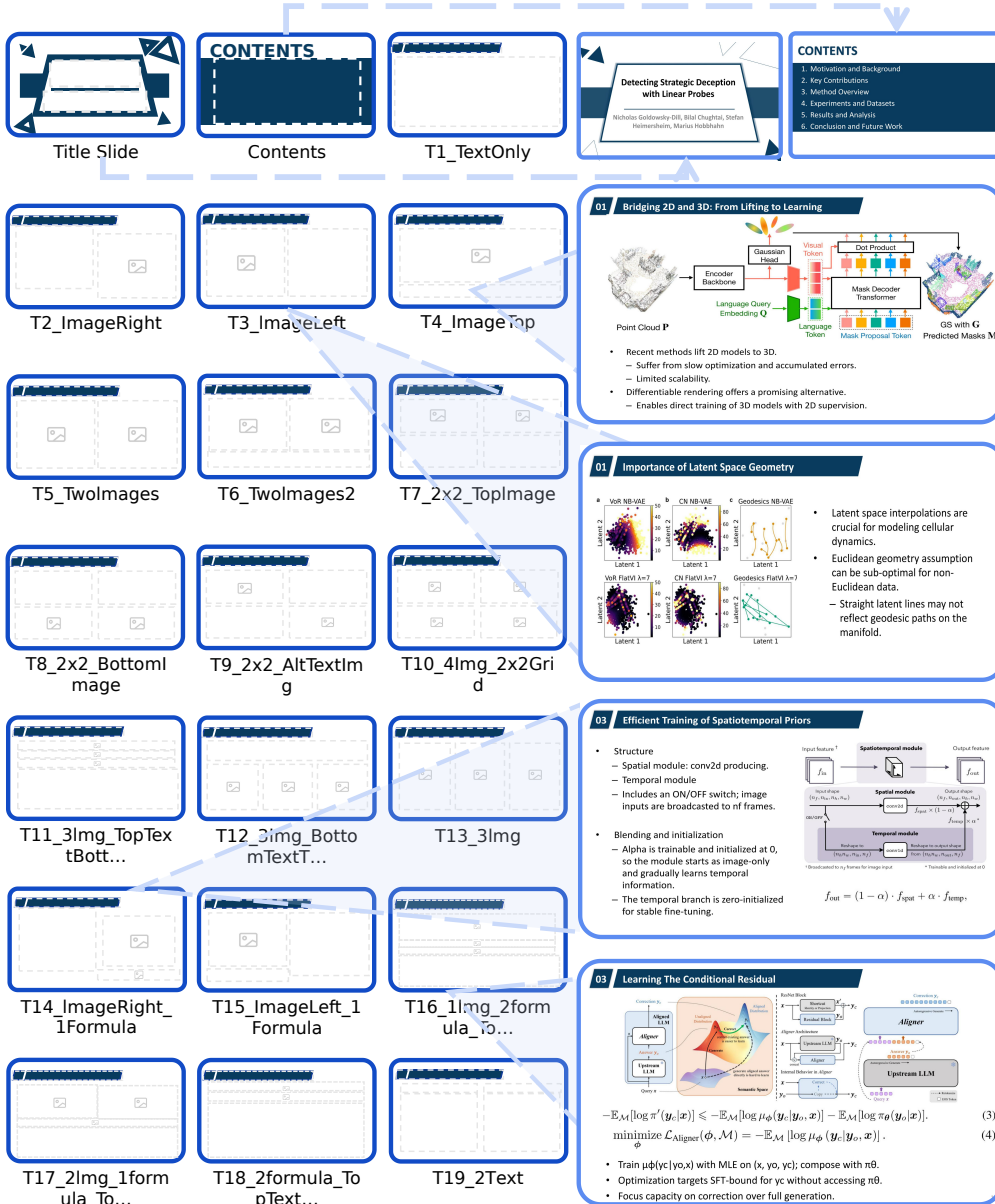


Figure 32 The complete slide template library used by the Arranger. Each template addresses a typical presentation structure, such as text-only, image-left, and two-column layouts.

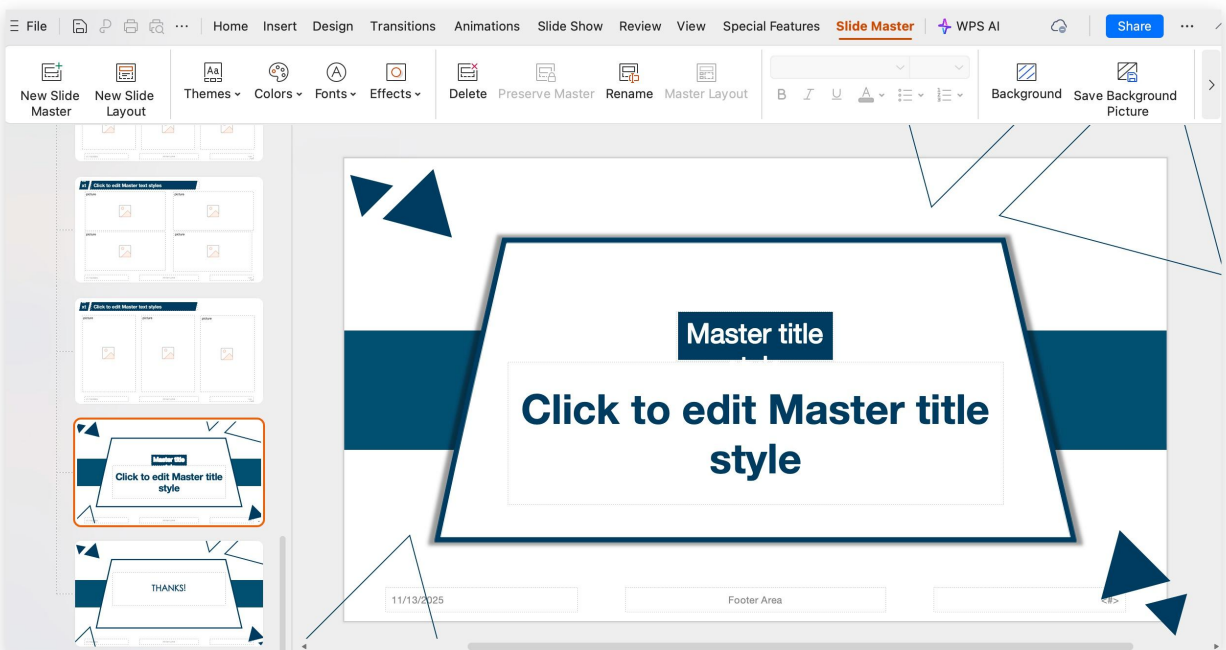


Figure 33 Slide Master interface in WPS. This screenshot illustrates the Slide Master view in WPS, where users can customize templates for SlideGen by defining fonts, colors, backgrounds, logos, and other design elements. Such flexibility enables users to create personalized slide designs for various themes and purposes.

Layout Agent

system_prompt:

You are SlidePlanBuilder.

Your ONLY task: return a single valid JSON object matching EXACTLY the schema below.

Do NOT include explanations, summaries, markdown code fences, or natural language.

template:

Instructions:

The PowerPoint canvas is **fixed at 13.3 in* 7.5 in** (16:9). You receive five JSON blobs:

1. **raw_result.json** - hierarchical summary of the paper. Structure:
2. **figures.json** - list of sections → subsections → visual assets. Example (keys may vary by paper):

Each 'imageN' or 'tableN' value is an index that maps to an image/table file name ('image_2.png', 'table_1.png', etc.).

3. **formula_index.json** - flat list of formula images:
4. **image_dims.json** - pixel dimensions for every 'image_.png'
5. **table_dims.json** - pixel dimensions for every 'table_.png'

What you must do for **every subsection**

1. **Pick the best slide template** from this library and output its 'template_id':

| ID | When to use |
|---------------------------------|---|
| T1_TextOnly | No images/tables |
| T2_ImageRight | 1 image + ≤4 bullets |
| T3_ImageLeft | Mirror of T2 (alternate left/right across consecutive slides) |
| T4_ImageTop | 1 wide image (aspect > 1.6) or table |
| T5_TwoImages | Exactly 2 side-by-side images, no text |
| T5_TwoImages2 | Two side-by-side images on top, with a text block below |
| T7_2x2_TopImage | 2*2 layout: top two blocks are images, bottom two are text |
| T8_2x2_BottomImage | 2*2 layout: top two blocks are text, bottom two are images |
| T9_2x2_AltTextImg | 2*2 layout: images on top-left & bottom-right, text on top-right & bottom-left |
| T10_4Img_2x2Grid | Four images arranged in a 2*2 grid, no text |
| T11_3Img_TopTextBottom | Vertically divided: 3 images on top, text block below |
| T12_3Img_BottomTextTop | Text block on top, 3 square images in one row below |
| T13_3Img | Title on top, followed by 3 evenly spaced images |
| T14_ImageRight_1Formula | Right column has two slots: top-right = one image or one table, bottom-right = one formula; left column = text bullets. Use when the slide has one key equation plus one main visual. |
| T15_ImageLeft_1Formula | Left column has two slots: top-left = one image or one table, bottom-left = one formula; right column = text bullets. Use when the slide has one key equation plus one main visual. |
| T16_1Img_2formula_TopTextBottom | Bottom = text block; top are three rows: row1 = one |

image or one table, row2 = one formula, row3 = one formula. Use for one main visual plus two formulas. |

| T17_2Img_1formula_TopTextBottom | Top row: two visuals side by side (each is one image or one table); middle row: one formula; bottom: text block. |

| T18_2formula_TopTextBottom | Top 2 rows: two formulas; bottom: text block. |

2. Generate hierarchical bullets summarising the subsection:

- Up to **6 top-level bullets**.
- Each top bullet may have **0-6 sub-bullets** (2-level outline).
- Top bullets ≤ 20 words; sub-bullets ≤ 25 words.

3. Select visuals that best support the bullets:

- **Formulas** belonging to the same subsection should stay **on the same slide whenever possible**; if more than 2, prefer 'T11_3Img_TopTextBottom'.
- **Do not crop or distort images** - preserve original aspect ratio (minor scaling to fit is fine).

4. Return a single valid JSON object with the exact schema below - do **NOT** wrap it in markdown.

```json

```
{
 "slides": [
 {
 "section": "<string>",
 "subsection": "<string>",
 "template_id": "T?_",
 "bullets": [
 {
 "text": "<string>",
 "sub": ["<string>", ...]
 }, ...
],
 "images": ["<filename>", ...],
 "tables": ["<filename>", ...],
 "formulas": ["<filename>", ...]
 }, ...
]
}
```

*Use the template-selection rules strictly so that downstream code can rely on them.*

Answer **only** with the JSON.

You **must** consider each visual's size and aspect ratio

*For every image / table, compute aspect = width ÷ height.*

*Choose the slide template and left/right/top placement based on aspect and absolute size:*

- **Wide** (aspect  $\geq 1.6$ ) → best placed across the top (template **T4\_ImageTop**), including wide tables.
- **Tall / square** (aspect  $\leq 1.0$ ) → best placed on the left or right (templates **T2\_ImageRight** or **T3\_ImageLeft**).
- If a visual's width is nearly the full slide width, prefer **T4\_ImageTop** to avoid excessive down-scaling.

*Never stretch or crop; only scale proportionally to fit placeholders.*

**Figure 34** Prompt for Arranger.

When designing slide layouts, you must carefully consider visual density and legibility constraints—especially for images that are wide or contain fine-grained details.

Such images often become unreadable when downscaled to fit dual-visual layouts like T2\_ImageRight, T3\_ImageLeft, or T5\_TwoImages2.

If multiple visuals(such as two images both with an aspect ratio greater than 1.6) are assigned to the same subsection but combining them would result in overcrowding or poor legibility, first check whether one of them fits better semantically in a neighboring subsection (e.g., covering a related topic or dataset). If so, move it to that subsection and assign a layout that presents it alone.

```
raw_result:
{{ raw_result_json }}
figures:
{{ figures_json }}
formulas:
{{ formulas_json }}
image_informations:
{{ image_informations_json }}
table_informations:
{{ table_informations_json }}

jinja_args:
- raw_result_json
- figures_json
- formulas_json
- image_informations_json
- table_informations_json
```

**Figure 35** Prompt for Arranger.

```

formula_match

system_prompt: |
You are an expert assistant tasked with assigning formulas to the most relevant paper sections.
You will be given:
1. JSON content of the paper structure, including sections and subsections (with title and
description).
2. A list of formulas with LaTeX, page_no, and the surrounding text context.
GOAL:
• Each formula should be assigned to its corresponding subsection, and a subsection may contain
multiple formulas.
• Produce a new JSON object that mirrors the structure of the provided paper_outline_json
(sections → subsections).
• For each subsection, assign zero, one, or multiple formulas.

• For each assigned formula, include:
 - "formulaN": <formula_id>
 - "reasonN": <reason string> explaining why it's assigned
• For each formula assigned to a subsection, generate a reason string ("reasonN") that not only
explains why the formula is assigned to this specific subsection,
 but also briefly interprets the formula's mathematical meaning or role within the paper.
• A formula may be assigned to multiple subsections (if conceptually appropriate), but not multiple
times in the same subsection.
• Keys must use correct suffixing: formula, formula1, formula2,... and reason, reason1, reason2, ...
• Keep section/subsection titles exactly as-is. Do not include their full content in the output.
• The final result should be a single valid JSON structure.

THINKING STRATEGY:
• Use the surrounding context and page_no from the formula list to guide assignment.
• Match concepts using keywords, notation, or nearby words (e.g., if the section talks about
"posterior", and the formula mentions $p(x|y)$, that's a match).
• Try to ensure each early-indexed formula (e.g. formula 1-5) is assigned at least once.
• Do not assign arbitrarily.

OUTPUT FORMAT:
{
 "sections": [
 {
 "title": "<Section Title>",
 "subsections": [
 {
 "title": "<Subsection Title>",
 "formula1": <id>,
 "reason1": "<explanation>",
 "formula2": <id>,
 "reason2": "<explanation>"
 },
 ...
]
 },
 ...
]
}

```

**Figure 36** Prompt for Formulizer.

```
}
```

**CAUTION:**

- Output must be valid JSON only (no comments or explanations).
- Only include sections/subsections where at least one formula is assigned.
- Match titles exactly from the original input.

template: |

Instructions:

1. Analyze the paper outline: {{ json\_content }}
2. Analyze the list of formulas with their latex and context: {{ formula\_information }}
3. For each subsection, decide which formulas (if any) are conceptually relevant based on content and wording.
4. Match carefully using terms, equations, symbols, and latent meaning.
5. Output a single JSON object following the system\_prompt rules.

jinja\_args:

- json\_content
- formula\_information

**Figure 37** Prompt for Formulizer.

## figure\_match

system\_prompt: |

You are an expert assistant tasked with assigning images and tables to the most relevant paper sections.

You will be given:

1. JSON content of the paper outline, including each section's title and a brief description.
2. A list of images (image\_information) with captions and size constraints.
3. A list of tables (table\_information) with captions and size constraints.

### GOAL

- Produce a JSON object that mirrors the hierarchy of paper\_outline\_json (sections → subsections).
- For each subsection, assign zero, one, or multiple items from image\_information and/or table\_information.
- Keys inside a subsection must follow:
  - image1, image2, ... with matching reason / reason1, ...
  - table1, table2, ... with matching reasonT1, reasonT2, ...
- The same image or table **may** appear in multiple subsections.
- Ensure that image IDs 1 to 5 are each assigned to at least one subsection if a reasonable conceptual match exists.
- If multiple images or tables match a section well, include all of them. Assign each item only once per section, using different keys: e.g., "image", "image1", "table", "table1", etc.
- If assigning an image, specify "image": <id>, where <id> is the identifier of the chosen image from "image\_information".
- If assigning a table, specify "table": <id>, where <id> is the identifier of the chosen table from "table\_information".
- Include an additional "reason", "reason1", etc. field briefly explaining why this assignment was made (e.g., how the image/table relates to the section content).
- If no image or table is assigned to a given section, omit that section from the final JSON (i.e., only list sections where you actually assign something).
- Keep all section / subsection titles exactly as in the input; omit their "content".

### IMPORTANT:

- The assignment should not be arbitrary. It must be logically consistent with the section's description and the provided caption for the image or table.
- Do not produce any layout properties or subsections here.
- The final output must be a single JSON object, mapping from section names to the chosen image/table ID plus the "reason" field.
- Extra note: If multiple images or tables are suitable, select the single best one and assign only that.
- If "image\_information" or "table\_information" is empty, you may end up assigning nothing to any section.

template: |

Instructions:

1. Read and analyze the paper's sections from {{ json\_content }} .
2. Look at {{ image\_information }} and {{ table\_information }}. Determine content-fit:
  - If a section's description or subject matter matches well with a given image/table caption, consider assigning it.
  - If multiple images or tables seem relevant, choose the single best fit.

**Figure 38** Prompt for Mapper.

- If none of the images or tables are relevant, or if none are provided, do not assign anything for that section.
- 3. Produce a single JSON object. Each key is the exact name of a top-level section (e.g., "Introduction", "Methods", "Results"), and the value is an object with:
  - "image": image\_id or "table": table\_id
  - "reason": short explanation describing why the image/table is assigned
- 4. If no assignment is made for a section, exclude that section from the JSON.
- 6. Ensure your final response strictly follows JSON syntax with no extra commentary.
- 7. Keep the original hierarchy (sections → subsections).
- 8. Use imageN / reason(N-1) and tableN / reasonTN naming as described.
- 9. No image/table reuse limits across subsections, but do not repeat an item twice inside the same subsection.

Example output format if two sections are assigned:

```
{
 "sections": [
 {
 "title": "Motivation And Background",
 "subsections": [
 {
 "title": "Challenges in Scientific Video Reconstruction",
 "image1": 1,
 "reason": "Image 1 illustrates sparse sampling and spatiotemporal gaps discussed in this subsection.",
 "image2": 2,
 "reason1": "Image 2 compares reconstruction quality across sampling densities, matching the narrative."
 },
 {
 "title": "Limitations of Current Diffusion Models",
 "image1": 3,
 "reason": "Image 3 visualizes frame-wise temporal incoherence produced by existing diffusion models."
 }
]
 },
 {
 "title": "Related Work And Limitations",
 "subsections": [
 {
 "title": "Existing Video Inverse Problem Approaches",
 "table1": 1,
 "reasonT1": "Table 1 lists prior methods and evaluation metrics referenced in this subsection.",
 "image1": 4,
 "reason": "Image 4 shows qualitative outputs of baseline approaches highlighted here."
 },
 {
 "title": "Plug-and-Play Diffusion Priors",
 "image1": 5,
 }
]
 }
]
}
```

**Figure 39** Prompt for Mapper.

"reason": "Image 5 presents an overview diagram of the PnPDP framework emphasized in this subsection."

```
 }
]
}
]
}
```

```
jinja_args:
- json_content
- image_information
- table_information
```

**Figure 40** Prompt for Mapper.

## Speaker Agent

```
system_prompt: |
You are a Speech-Generation agent.
Your task is to read the supplied document ('`json_content`' and '`raw_result`') and
generate **a spoken script** that summarizes each subsection of the document.
Every paragraph should be clear, concise, and suitable for a conference talk.

Instructions:
1. Read the JSON content in '`json_content`' and the original text in '`raw_result`' closely.
2. Write one spoken paragraph for each subsection. Each paragraph should be:
 - 2 to 5 sentences long.
 - Focused on providing a high-level summary of the subsection.
 - Avoid unnecessary technical jargon and be suitable for an audience with general scientific knowledge.
3. Keep the content **factual** and **to the point**, summarizing the subsection without adding inference.
4. Do not use **em dashes** or **hyphens** to link clauses.
5. Each subsection should have a corresponding paragraph, and each paragraph should correspond directly to one
subsection.
6. Do not include any citations, references, or exact numerical data.
7. The output should be in **JSON format** with the following strict schema:

template: |
=====
INSTRUCTIONS
=====
1. Read both the JSON content in '`json_content`' and the raw document in '`raw_result`' carefully.
2. Write one spoken paragraph for each subsection in the document.
 - Paragraphs should summarize the content of each subsection in a clear and concise manner.
 - Each paragraph should be 2 to 5 sentences long.
 - The writing should be suitable for a spoken presentation at a conference.
 - Avoid technical terms unless necessary, and provide brief explanations if required.
3. Ensure the text remains **factual** and **brief** without adding any new information.
4. Do not use **em dashes** or **hyphens** as punctuation.
5. Output **strictly** in JSON format with the following structure:

Output JSON schema (strict):
{
 "speaker_script": [
 {
 "section_index": <integer, zero-based>,
 "section_title": "<string>",
 "subsections": [
 {
 "subsection_index": <integer, zero-based>,
 "subsection_title": "<string>",
 "script": "<one paragraph with 2 to 5 sentences, no em dashes, no hyphenated clause joining>"
 }
]
 },
 "meta": {
 "language": "en",
 "style": "conference talk, clear and engaging",
 "version": "v1"
 }
]
}

jinja_args:
- json_content
- raw_result
```

**Figure 41** Prompt for Speaker.

## Refiner

```
system_prompt: |
You are the ColorRefiner agent in our SlideGen pipeline.
Your role:
- You receive (1) a baseline set of HSV adjustment parameters and (2) a natural-language style description for the slide theme.
- You DO NOT generate colors directly. Instead, you slightly refine the numeric parameters that control a deterministic HSV-space adjustment function.
- The goal is to better match the desired style while keeping parameters in a safe, reasonable range.
template: |
Context:
- Our color pipeline first extracts a base RGB theme color from images (e.g., logos or key figures).
- Then we apply a deterministic function 'move_right_then_down_adaptive' in HSV space, controlled by the following parameters:
 - satTarget: target saturation we gently push S toward
 - satFloor: minimum allowed saturation
 - satCap: maximum allowed saturation
 - targetV: target brightness level for a dark theme
 - vCap: maximum brightness after adjustment
 - gamma: strength of the adaptive darkening above targetV
 - fallbackHue: hex color used when the original color is nearly gray
Current baseline parameters (already working but not yet style-optimized) are:
{
 "satTarget": 0.80,
 "satFloor": 0.70,
 "satCap": 0.99,
 "targetV": 0.40,
 "vCap": 0.99,
 "gamma": 3.8,
 "fallbackHue": "#2B5FA6"
}

Your task:
- Given the baseline parameters above and the following style description:
 STYLE_DESCRIPTION: "dark academic, calm, professional"
- Propose a slightly refined parameter set that:
 - keeps values in reasonable ranges:
 - satTarget, satFloor, satCap $\in [0.0, 1.0]$
 - targetV, vCap $\in [0.0, 1.0]$
 - gamma $\in [0.0, 10.0]$
 - does NOT deviate too far from the baseline (think of small, stylistic nudges, not drastic changes).
 - maintains a dark theme suitable for white or near-white text.
 - avoids overly neon or over-saturated colors.
 - keeps fallbackHue close to a desaturated, trustworthy blue, unless the style clearly suggests otherwise.
Output format:
- Return ONLY a valid JSON object with the following keys:
 - "satTarget": float
 - "satFloor": float
 - "satCap": float
 - "targetV": float
 - "vCap": float
 - "gamma": float
 - "fallbackHue": string (hex color, like "#2B5FA6")
- Do not include explanations, comments, or any extra text outside the JSON.
```

**Figure 42** Prompt for Refiner.

## Outline JSON

```
{
 "metadata": {
 "title": "A Touch, Vision, and Language Dataset for Multimodal Alignment",
 "author": "Letian Fu; Gaurav Datta; Huang Huang; William Chung-Ho Panitch; Jaimyn Drake;
 Joseph Ortiz; Mustafa Mukadam; Mike Lambeta; Roberto Calandra; Ken Goldberg",
 "publish date": "2024",
 "organization": "UC Berkeley; Meta AI; TU Dresden"
 },
 "sections": [
 {
 "title": "Motivation: Why Integrate Touch With Vision And Language?",
 "subsections": [
 {
 "title": "Gaps In Multimodal Models",
 "content": "Most multimodal generative and alignment models focus on visual, textual, and sometimes audio or action signals, leaving tactile sensing underexplored. Yet touch captures material, texture, compliance, and force-related semantics vital for manipulation and human-like perception. A lack of open-vocabulary tactile-language data and difficulty synchronizing tactile with visual context impede progress. This work addresses scarce labels, subjective descriptions, and misalignment by proposing a dataset and models that align tactile, visual, and linguistic representations."
 },
 {
 "title": "Why Does This Matter?",
 "content": "Combining touch with vision and language can yield agents that more robustly infer material properties and contact states, improving open-vocabulary understanding and manipulation. The approach promises better generalization than vision-only models, enabling text-grounded tactile understanding and generation. It may benefit robotics, haptics research, and broader multimodal AI by providing a scalable path to tactile-language supervision via pseudo-labels."
 }
]
 },
 {
 "title": "Related Work And Limitations Of Existing Approaches",
 "subsections": [
 {
 "title": "Multimodal Encoders And Alignment",
 "content": "CLIP and derivatives align vision and language using contrastive learning; ImageBind extends to more modalities but primarily binds them through vision. Other works include masked multimodal pretraining and parameter-efficient alignment with LLMs. However, direct tactile-language alignment is typically absent, and tactile is often only bound to vision, limiting tactile semantic coverage."
 },
 {
 "title": "Tactile Perception And Datasets",
 "content": "Prior tactile-vision efforts address closed-set material or cloth classification and manipulation, often in lab settings, with limited vocabulary and diversity. Some datasets integrate audio or point clouds, but open-vocabulary tactile-language labels are missing. Concurrent efforts bind touch to vision without finetuning LLMs, leaving room for stronger tactile-language alignment"
 }
]
 }
]
}
```

**Figure 43** Output JSON of Outliner Agent.

## Outline JSON

```
and generation."
 },
 {
 "title": "Training From Pseudo-Labels",
 "content": "Self-training and pseudo-labeling reduce annotation costs. Recent LLM/VLM pipelines use GPT-generated instruction data, but typically with matching input-output modalities. Here, vision-only GPT-4V generates tactile descriptions from images to supervise alignment with tactile data, expanding labeled coverage while acknowledging potential label noise."
 }
]
},
{
 "title": "Key Contributions Of This Work",
 "subsections": [
 {
 "title": "TVL Dataset: 44K Vision\u2013Tactile\u2013Language Triplets",
 "content": "A new dataset with 43,741 in-contact vision\u2013tactile pairs and open-vocabulary labels: 10% human-annotated (SSVTP) and 90% GPT-4V pseudo-labeled (HCT). The dataset spans in-the-wild settings, synchronized acquisition, and 254 unique tactile adjectives. A 99%/1% split is used with a human-labeled test set."
 },
 {
 "title": "Vision- And Language-Aligned Tactile Encoder",
 "content": "A tactile encoder trained via pairwise contrastive learning across tactile\u2013language, tactile\u2013vision, and vision\u2013language pairs, aligning tactile inputs directly to CLIP\u2019s latent space. Training strategies include inclusion of background (no-contact) frames labeled as \u2018background,\u2019 projector removal for vision/text, and randomized adjective subsets to improve robustness."
 },
 {
 "title": "TVL-LLaMA: Touch\u2013Vision\u2013Language Generation",
 "content": "A multimodal generation model finetuning LLaMA2-7B with TVL encoders to produce tactile descriptions from tactile and visual inputs. Two-stage training follows ImageBind-LLM style fusion, with additional instruction data (LLaVA CC3M, Alpaca, LLaVA 150K) to counter safety refusals and improve instruction-following."
 }
]
},
{
 "title": "Dataset: Collection, Cleaning, And Language Labeling",
 "subsections": [
 {
 "title": "Hardware And Synchronous Data Collection",
 "content": "A 3D-printed handheld rig integrates a DIGIT tactile sensor and a Logitech BRIO webcam to capture synchronized tactile and visual streams at 30 Hz during approach, contact, slide, and withdrawal trajectories. Five human collectors gathered 20 hours of diverse in-the-wild interactions ensuring the contact region remains in view, boosting variety and alignment fidelity."
 },
 {

```

**Figure 44** Output JSON of Outliner Agent.

## Outline JSON

```
{
 "title": "Cleaning: Contact Versus No-Contact Frames",
 "content": "Using a pretrained tactile encoder, frames are categorized by cosine
similarity to a background embedding; contact is flagged when similarity drops below 0.6. The final
dataset includes 43,741 in-contact and 169,292 out-of-contact pairs. Contact frames are used
primarily for training alignment and evaluation; a portion of no-contact frames aids generalization."
,
 {
 "title": "Language Labeling: Human And GPT-4V Pseudo-Labels",
 "content": "SSVTP pairs are human-labeled using up to five adjectives drawn from a
curated 400-word tactile vocabulary. HCT labels are generated by GPT-4V using both full and
cropped images around the contact. Failures (e.g., occlusions, blur) are mitigated by labeling nearby
frames within a trajectory or dropping unlabeled trajectories. Overall, 39,154 pseudo-labeled images
are produced."
,
 {
 "title": "Dataset Statistics And Split",
 "content": "SSVTP: 4,587 pairs; HCT: 39,154 in-contact and 169,292 no-contact pairs
across 1,486 trajectories. A 99/1 train-test split is used; the test set (402 pairs) is human-labeled. GPT-
4V averages 4.25 adjectives per item vs. 2.70 for humans, covering 254 distinct descriptors and
yielding a long-tailed vocabulary distribution."
 }
}
},
{
 "title": "Method Overview And Technical Design",
 "subsections": [
 {
 "title": "Contrastive Alignment Across All Modality Pairs",
 "content": "Unlike ImageBind\u2019s vision-centric binding, TVL optimizes InfoNCE
across tactile\u2013language, tactile\u2013vision, and vision\u2013language. The tactile encoder
(ViT-Tiny/Small/Base) is randomly initialized and projects to CLIP\u2019s latent space; vision/text
use frozen OpenCLIP without additional projectors. Training shuffles and subsets language adjectives
per sample for label diversity and includes 10% no-contact frames labeled \u2018background\u2019
to curb overfitting."
 },
 {
 "title": "Instruction Tuning With Multimodal Tokens",
 "content": "TVL-LLaMA follows ImageBind-LLM/LLaMA-Adapter fusion, averaging
vision and tactile latents into a single token and using a zero-initialized gate and LoRA for efficient
alignment. Pretraining uses LLaVA CC3M subset and TVL (empty tactile image for CC3M),
followed by finetuning on TVL, Alpaca, and LLaVA 150K to improve instruction following and
safety-guarded refusals."
 },
 {
 "title": "Prompting And Preprocessing Choices",
 "content": "Prompts are diversified for tactile description generation during fine-tuning;
evaluation uses GPT-4 grading prompts with order randomization to reduce bias."
 }
]
}
```

**Figure 45** Output JSON of Outliner Agent.

## Outline JSON

Tactile preprocessing includes padding, resizing to 224x224, optional background subtraction, and normalization. Vision preprocessing uses CLIP statistics and tailored crops to keep sensor contact visible, matching GPT-4V labeling conditions."

```
 }
],
},
{
 "title": "Experiments, Datasets, And Evaluation Protocols",
 "subsections": [
 {
 "title": "Open-Vocabulary Cross-Modal Classification",
 "content": "On the human-labeled TVL test set (402-way), top-1/top-5 accuracy is computed for tactile vision and tactile language. To handle synonymy and order sensitivity in CLIP text embeddings, a synonym-expanded label set is built via GPT-4; cosine similarity thresholds define correctness. Vision text uses OpenCLIP scores. Baselines include SSVTP encoders and CLIP."
 },
 {
 "title": "TVL Benchmark For Tactile Description Generation",
 "content": "Given full image, cropped image, and tactile frame, models output up to five adjectives. GPT-4 scores responses against human labels from 1 to 10 with rationales. Models compared include GPT-4V, LLaVA variants, ViP-LLaVA, LLaMA-Adapter, BLIP-2, InstructBLIP, SSVTP-LLaMA, and TVL-LLaMA (Tiny/Small/Base). Statistical significance is assessed via paired t-tests."
 },
 {
 "title": "Additional Tasks And Ablations",
 "content": "A zero-shot binary object category test (fabric vs. plastic) illustrates downstream utility. Ablations analyze encoder size, disabling tactile text loss, modality removal, no-contact data mixing, prompt variants, background subtraction, training subsets (SSVTP vs. HCT vs. TVL), and freezing vs. finetuning the LLM. Overfitting to pseudo-labels and distribution shift between human and GPT-4V labels are examined."
 }
],
},
{
 "title": "Results And Comparative Analysis",
 "subsections": [
 {
 "title": "Classification Performance",
 "content": "TVL tactile encoders achieve strong tactile vision (up to 81.7% top-1) and tactile text (up to 36.7% top-1) accuracy on the TVL test set, outperforming SSVTP on in-the-wild data and surpassing OpenCLIP's vision text alignment for tactile semantics. Direct tactile text supervision is crucial; removing it reduces tactile text accuracy markedly."
 },
]
}
```

**Figure 46** Output JSON of Outliner Agent.

## Outline JSON

```
{
 "title": "TVL Benchmark: Generation Scores",
 "content": "TVL-LLaMA outperforms GPT-4V by at least 12% and open-source VLMs by larger margins, with significant p-values. Improvements hold across SSVTP (lab) and HCT (in-the-wild) subsets, showing benefits from limited human labels and extensive pseudo-labels. SSVTP-LLaMA, lacking tactile\u2013text pretraining, underperforms, underscoring the need for explicit tactile-language alignment."
},
{
 "title": "Ablation Insights And Sensitivity",
 "content": "Including all modality pair losses boosts alignment; background subtraction and limited no-contact data mitigate overfitting and improve downstream scores. Encoder size trades off robustness and overfitting to pseudo-labels. Prompt format has minor effects. Freezing the LLM can match finetuning in some settings, suggesting strong encoder alignment to language space."
},
],
,
{
 "title": "Limitations, Conclusion, And Future Directions",
 "subsections": [
 {
 "title": "Current Limitations",
 "content": "Vision-derived pseudo-labels may misdescribe tactile sensations when contact is occluded or ambiguous. Distribution shifts between GPT-4V pseudo-labels and human test labels can cause overfitting or evaluation gaps. Safety tuning in LLaMA2 required additional instruction data to avoid refusals. The vocabulary distribution is long-tailed with some noisy descriptors."
 },
 {
 "title": "Conclusion And Broader Impact",
 "content": "TVL provides a large-scale, synchronized vision\u2013tactile dataset with open-vocabulary labels, enabling a tactile encoder aligned with both vision and language and a TVL-LLaMA capable of generating tactile descriptions. Results demonstrate improved tactile-vision-language alignment and generation over strong baselines. The work advances embodied AI and robotic manipulation through richer multimodal grounding."
 },
 {
 "title": "Future Work",
 "content": "Scale human-labeled coverage, diversify environments and sensors, improve pseudo-label uncertainty handling, and explore richer task formulations (e.g., action-conditioned tactile reasoning). Investigate better fusion strategies beyond latent averaging, domain adaptation for occlusion or lighting, and extended downstream tasks such as open-world material and affordance understanding."
 }
]
}
```

**Figure 47** Output JSON of Outliner Agent.

### Arranger JSON for images and tables

```
{
 "slides": [
 {
 "section": "Introduction to Prompt Caching",
 "subsection": "Introduction to Prompt Caching",
 "template_id": "T4_ImageTop",
 "bullets": [
 {
 "text": "Prompt caching leads to data-dependent timing variations.",
 "sub": [
 "Cached prompts are processed faster than non-cached ones.",
 "This can result in side-channel timing attacks."
]
 },
 {
 "text": "Shared caches across users increase privacy risks.",
 "sub": [
 "If caches are shared, attackers can infer prompt information."
]
 }
],
 "images": [
 "Auditing_Prompt_Caching_in_Language_Model_APIs-picture-1.png"
],
 "tables": [],
 "formulas": []
 },
 {
 "section": "Introduction to Prompt Caching",
 "subsection": "Risks of Timing Attacks",
 "template_id": "T1_TextOnly",
 "bullets": [
 {
 "text": "Timing differences can be exploited by attackers.",
 "sub": [
 "Attackers can infer information about other users' prompts.",
 "Global cache sharing poses significant privacy concerns."
]
 }
],
 "images": [],
 "tables": [],
 "formulas": []
 },
 {
 "section": "Preliminaries and Assumptions",
 "subsection": "Understanding Prompt Caching",
 "template_id": "T4_ImageTop",
 "bullets": [
]
]
}
```

**Figure 48** Output JSON of Arranger Agent.

### Arranger JSON for images and tables

```
{
 "text": "Prompt caching reuses attention KV cache in Transformer LLMs.",
 "sub": [
 "Cache hits occur when prompts share a prefix with cached prompts.",
 "This results in faster processing times."
]
},
{
 "images": [
 "Auditing_Prompt_Caching_in_Language_Model_APIs-picture-1.png"
],
 "tables": [],
 "formulas": []
},
{
 "section": "Preliminaries and Assumptions",
 "subsection": "API Assumptions",
 "template_id": "T1_TextOnly",
 "bullets": [
 {
 "text": "Arbitrary prompts can be sent to the API.",
 "sub": [
 "Time to first token (TTFT) can be measured.",
 "Timing variations indicate caching."
]
 }
],
 "images": [],
 "tables": [],
 "formulas": []
},
{
 "section": "Preliminaries and Assumptions",
 "subsection": "Levels of Cache Sharing",
 "template_id": "T4_ImageTop",
 "bullets": [
 {
 "text": "Cache sharing occurs at different levels.",
 "sub": [
 "Per-user, per-organization, or globally.",
 "Global caching poses the highest privacy risk."
]
 }
],
 "images": [
 "Auditing_Prompt_Caching_in_Language_Model_APIs-picture-2.png"
],
 "tables": [],
 "formulas": []
},
}
```

**Figure 49** Output JSON of Arranger Agent.

## Arranger JSON for images and tables

```
{
 "section": "Audit Methodology",
 "subsection": "Audit Formulation",
 "template_id": "T11_3Img_TopTextBottom",
 "bullets": [
 {
 "text": "Audit is a statistical hypothesis test.",
 "sub": [
 "Detects prompt caching and cache sharing level.",
 "Compares response time distributions for cache hits and misses."
]
 }
],
 "images": [
 "Auditing_Prompt_Caching_in_Language_Model_APIs-picture-3.png",
 "Auditing_Prompt_Caching_in_Language_Model_APIs-picture-4.png"
],
 "tables": [],
 "formulas": [
 "Auditing_Prompt_Caching_in_Language_Model_APIs-formula-1.png"
]
},
{
 "section": "Audit Methodology",
 "subsection": "Audit Implementation Details",
 "template_id": "T1_TextOnly",
 "bullets": [
 {
 "text": "Audit uses configuration parameters like prompt length.",
 "sub": [
 "Involves sending prompts to produce cache hits and misses.",
 "Statistically tests for response time differences."
]
 }
],
 "images": [],
 "tables": [],
 "formulas": []
},
{
 "section": "Auditing Real-World APIs",
 "subsection": "Audit Results",
 "template_id": "T4_ImageTop",
 "bullets": [
 {
 "text": "Prompt caching detected in 8 out of 17 API providers.",
 "sub": [
 "Global cache sharing identified in 7 providers.",
 "Potential privacy leakage as attackers infer prompt information."
]
 }
]
}
```

**Figure 50** Output JSON of Arranger Agent.

### Arranger JSON for images and tables

```
 }
],
 "images": [],
 "tables": [
 "Auditing_Prompt_Caching_in_Language_Model_APIs-table-1.png"
],
 "formulas": []
},
{
 "section": "Leakage of Architecture Information",
 "subsection": "Architecture Information Leakage",
 "template_id": "T4_ImageTop",
 "bullets": [
 {
 "text": "Prompt caching reveals model architecture information.",
 "sub": [
 "Cache hits between matching prefixes indicate decoder-only architecture."
]
 }
],
 "images": [
 "Auditing_Prompt_Caching_in_Language_Model_APIs-picture-1.png"
],
 "tables": [],
 "formulas": []
},
{
 "section": "Mitigations and Recommendations",
 "subsection": "Mitigations for Privacy Leakage",
 "template_id": "T4_ImageTop",
 "bullets": [
 {
 "text": "Implement per-user caching to prevent privacy leakage.",
 "sub": [
 "Providers should disclose caching policies.",
 "Users need information to make informed decisions."
]
 }
],
 "images": [
 "Auditing_Prompt_Caching_in_Language_Model_APIs-picture-2.png"
],
 "tables": [],
 "formulas": []
},
{
 "section": "Mitigations and Recommendations",
 "subsection": "Disabling Caching",
 "template_id": "T1_TextOnly",
 "bullets": [
 {
 "text": "Disabling caching is a simple mitigation for privacy leakage, but it may impact performance and user experience.".
 "sub": [
 "It is important to carefully consider the trade-offs between privacy and performance when disabling caching.".
 "Users should be informed about the implications of disabling caching and given the option to enable it if desired."
]
 }
],
 "images": [
 "Auditing_Prompt_Caching_in_Language_Model_APIs-picture-3.png"
],
 "tables": [],
 "formulas": []
}
```

**Figure 51** Output JSON of Arranger Agent.

### Arranger JSON for images and tables

```
"bullets": [
 {
 "text": "Disabling caching prevents information leakage.",
 "sub": [
 "May eliminate performance benefits.",
 "Providers must balance privacy with performance."
]
 }
],
"images": [],
"tables": [],
"formulas": []
},
{
 "section": "Conclusion and Future Work",
 "subsection": "Conclusion and Future Work",
 "template_id": "T1_TextOnly",
 "bullets": [
 {
 "text": "Prompt caching can lead to privacy and information leakage.",
 "sub": [
 "Future work should evaluate security and privacy of ML systems."
]
 }
],
"images": [],
"tables": [],
"formulas": []
}
]
```

**Figure 52** Output JSON of Arranger Agent.

## Speaker JSON

```
{
 "speaker_script": [
 {
 "section_index": 0,
 "section_title": "Overview",
 "subsections": [
 {
 "subsection_index": 0,
 "subsection_title": "Introduction",
 "script": "This study explores how a new system improves efficiency and reliability across key tasks. We compare current practices with a proposed approach and highlight measurable gains. The goal is to provide practical insights that teams can apply without major disruption."
 },
 {
 "subsection_index": 1,
 "subsection_title": "Contributions",
 "script": "Our work delivers three main outcomes. First, we present a streamlined method that reduces time and complexity. Second, we offer a clear evaluation on realistic data. Third, we share guidance to help others reproduce the results."
 }
]
 },
 {
 "section_index": 1,
 "section_title": "Method",
 "subsections": [
 {
 "subsection_index": 0,
 "subsection_title": "Design",
 "script": "The method follows a simple pipeline with well defined steps. Inputs are cleaned, processed, and then combined to produce a final output. Each step uses standard tools so teams can adopt the method with minimal change."
 },
 {
 "subsection_index": 1,
 "subsection_title": "Implementation",
 "script": "We implemented the approach with off the shelf libraries and a small amount of custom code. The system runs on common hardware and scales to larger workloads through batching. Configuration is kept minimal to reduce setup time."
 }
]
 },
 {
 "section_index": 2,
 "section_title": "Evaluation",
 "subsections": [
 {
 "subsection_index": 0,
 "subsection_title": "Setup",
 "script": "The evaluation is conducted using a comprehensive set of benchmarks and real-world data. We compare the proposed system against existing methods in terms of performance, resource utilization, and user satisfaction. The results show significant improvements in all metrics, validating the proposed approach."
 }
]
 }
]
}
```

**Figure 53** Output JSON of Speaker Agent.

## Speaker JSON

```
"script": "We evaluated the system on a representative dataset and realistic scenarios. Baselines include widely used methods to ensure a fair comparison. Metrics focus on accuracy, speed, and resource use."
},
{
 "subsection_index": 1,
 "subsection_title": "Results",
 "script": "Results show consistent gains in accuracy and substantial time savings. The system maintains performance under higher load and uses fewer resources. These improvements hold across different input sizes and conditions."
},
{
 "subsection_index": 2,
 "subsection_title": "Ablation",
 "script": "We removed components one at a time to understand their impact. Key modules contributed most of the gains while some steps offered smaller benefits. This analysis informs where to focus effort for future tuning."
}
],
},
{
 "section_index": 3,
 "section_title": "Discussion",
 "subsections": [
 {
 "subsection_index": 0,
 "subsection_title": "Strengths and Limitations",
 "script": "The approach is easy to deploy and delivers strong performance across tasks. It relies on standard tools which helps adoption, but it may need adjustments for niche data. Future work will address these edge cases and extend coverage."
 },
 {
 "subsection_index": 1,
 "subsection_title": "Use Cases",
 "script": "This method suits teams seeking quick wins without heavy redesign. It can support batch processing, near real time tasks, and routine analytics. Organizations can start small and scale as confidence grows."
 }
],
},
{
 "section_index": 4,
 "section_title": "Conclusion",
 "subsections": [
 {
 "subsection_index": 0,
 "subsection_title": "Summary",
 "script": "We presented a practical method that improves accuracy, speed, and efficiency. The evaluation confirms robust gains across settings with simple deployment. We hope these findings help teams achieve results quickly."
 }
]
}
```

**Figure 54** Output JSON of Speaker Agent.

### Speaker JSON

```
},
{
 "subsection_index": 1,
 "subsection_title": "Future Work",
 "script": "Next steps include broader benchmarks, automated tuning, and stronger monitoring. We plan to release tools that simplify setup and ongoing maintenance. Collaboration invitations are open to validate the method in new domains."
}
],
"meta": {
 "language": "en",
 "style": "conference talk, clear and engaging",
 "version": "v1"
}
}
```

**Figure 55** Output JSON of Speaker Agent.

## Mapper JSON for images and tables

```
{
 "sections": [
 {
 "title": "Proposed Method: Multi-Turn Program Synthesis",
 "subsections": [
 {
 "title": "Multi-Turn Approach",
 "image1": 1,
 "reason": "Image 1 provides an illustrative example of the Multi-Turn Programming Benchmark, which aligns with the multi-turn approach described in this subsection."
 },
 {
 "title": "Advantages of Multi-Turn Synthesis",
 "table1": 3,
 "reasonT1": "Table 3 shows evaluation results on the Multi-Turn Programming Benchmark, directly related to the advantages of multi-turn synthesis discussed here."
 },
 {
 "title": "Experiments and Evaluation",
 "subsections": [
 {
 "title": "Single-Turn Evaluation",
 "table1": 1,
 "reasonT1": "Table 1 presents evaluation results on the HumanEval benchmark, relevant to the single-turn evaluation discussed in this subsection."
 },
 {
 "title": "Multi-Turn Evaluation",
 "image1": 2,
 "reason": "Image 2 shows the difference in pass rates between single-turn and multi-turn formulations, which is pertinent to the multi-turn evaluation."
 },
 {
 "title": "Results and Analysis",
 "subsections": [
 {
 "title": "Performance on Benchmarks",
 "table1": 4,
 "reasonT1": "Table 4 compares multi-turn and single-turn specifications, which is relevant to the performance analysis on benchmarks."
 },
 {
 },
],
 },
],
 },
],
 },
],
}
```

**Figure 56** Output JSON of Mapper Agent.

```
{
 "title": "Model Training and Datasets",
 "subsections": [
 {
 "title": "Datasets Used",
 "table1": 7,
 "reasonT1": "Table 5 provides statistics for training corpora, which is relevant to the datasets used for training CODEGEN models."
 }
]
}
```

**Figure 57** Output JSON of Mapper Agent.

Formulizer JSON

```
{
 "sections": [
 {
 "title": "Method Overview",
 "subsections": [
 {
 "title": "Similarity Function Choices",
 "formula1": 1,
 "reason1": "The formula '\sin (t - m), q' is related to the similarity functions discussed in this subsection, specifically focusing on different ways to measure similarity between neuron activations and concept matrices. This aligns with the exploration of various similarity functions like cosine similarity and SoftWPMI."
 }
]
 }
]
}
```

**Figure 58** Output JSON of Formulizer Agent.